Proton's isovector PDF with updated analysis of large-momentum lattice data

Xiangdong Ji, Yushan Su

arXiv:2606.22224

Outline

Benchmark of LaMET	Proton unpolarized isovector PDF as a benchmark to evaluate LaMET's x-dependence calculation; Previous works: lattice artifacts and less-advanced theoretical analysis lead to inconsistent results among lattice groups and many deviate from phenomenological PDFs.
Reanalysis of lattice datasets	Incorporating all the latest theoretical tools; Mitigating lattice artifacts empirically.
LaMET results compared with global fit	The variations among lattice groups are dramatically reduced; The physical-limit result is consistent with global fit PDF within $\sim 1\sigma$.

Outline

Benchmark of LaMET

Proton unpolarized isovector PDF as a benchmark to evaluate LaMET's x-dependence calculation;
Previous works: lattice artifacts and less-advanced theoretical analysis lead to inconsistent results among lattice groups and many deviate from phenomenological PDFs.

Reanalysis of lattice datasets

Incorporate [illegible] theoretical tools;
Mitigate lattice artifacts [illegible].

LaMET results compared with global fit

The variations among lattice groups are dramatically reduced;
The physical-limit result is consistent with global fit PDF within $\sim 1\sigma$.

EFT and high-energy collision

- An EFT: retains specific dofs from the full theory, while integrating out the others.
- QCD factorization viewed as EFT
  - A field can be decomposed

    e.g. $\psi = \psi_{\text{high}} + \psi_{\text{low}}$ Ji:2024oka
  - Cross sections are factorized into UV (high energy) and IR (low energy) parts:

    $\sigma = \text{UV} * \text{IR} + \cdots$

    UV: experimental probes&final state interactions, perturbatively calculable

    IR: internal hadronic structures, non-perturbative physics

    ...: power corrections suppressed in the high energy limit
- How to formulate the low energy EFT?

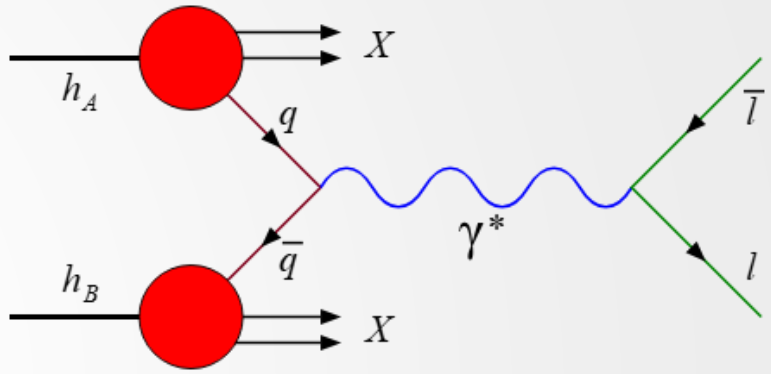

Wikipedia: Drell–Yan process

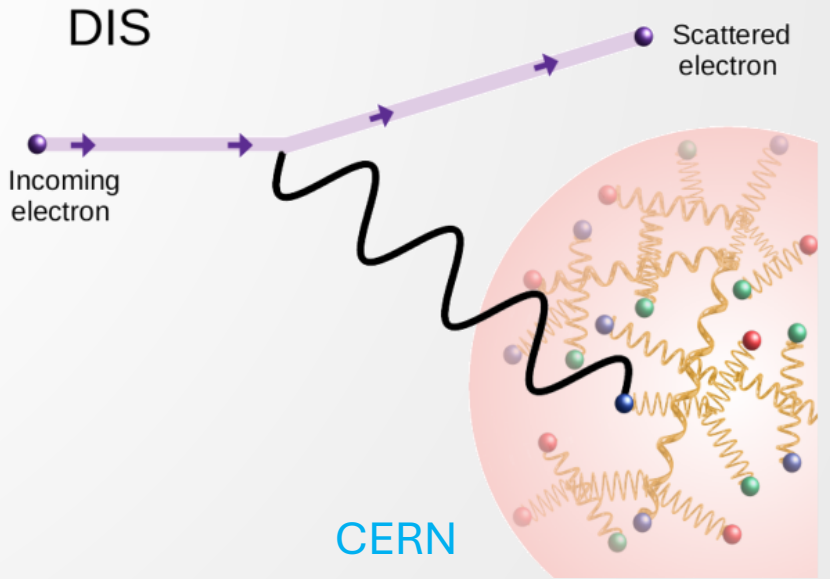

CERN

LaMET for x-dependence calculation of PDF

- Collinear modes along the light-cone (Collins_2023,Stewart:2013SCETnotes,Becher:2014oda): parton distribution function (PDF)

$$f(x,\mu) = \int \frac{d\xi^-}{4\pi} e^{-i\,\xi^- P^+ x} \langle P|\bar{\psi}(\xi^-) U(\xi^-,0)\gamma^+\psi(0)|P\rangle$$

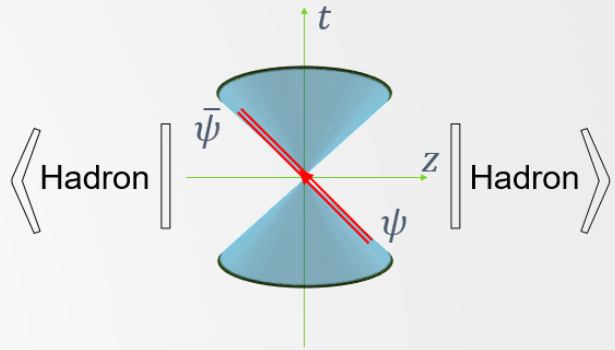

Beauty: momentum density interpretation

Issue: cannot be simulated on a Euclidean lattice

- Collinear modes selected by the hadron velocity (Ji:2013dva,Ji:2014gla,Ji:2020byp,Ji:2022ezo,Ji:2024oka): longitudinal momentum distribution (LMD)

$$\tilde{f}(y,P^z) = \int \frac{dz}{4\pi} e^{\mathrm{i}\,z\,P^z y} \langle P|\bar{\psi}(z)\gamma^t U(z,0)\psi(0)|P\rangle$$

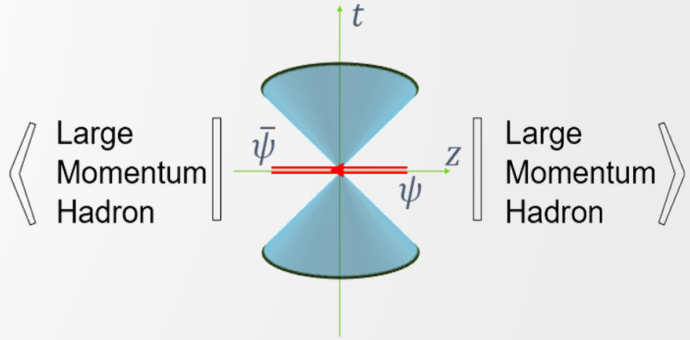

measurable in lattice QCD

- Large momentum expansion (Ji:2024oka)

$$f(x,\mu) = \int \frac{dy}{|y|} C\left(\frac{x}{y}, \frac{\mu}{|y|P^z}\right) \tilde{f}(y,P^z) + O\left(\frac{\Lambda^2_{\mathrm{QCD}}}{x^2P_z^2}, \frac{\Lambda^2_{\mathrm{QCD}}}{(1-x)^2P_z^2}\right)$$

which allows **a direct x-dependence calculation of PDF with controlled precision**

Benchmark: proton unpolarized isovector PDF

- Measured in high precision from experiments: numerous datasets; no mixing with gluon channel

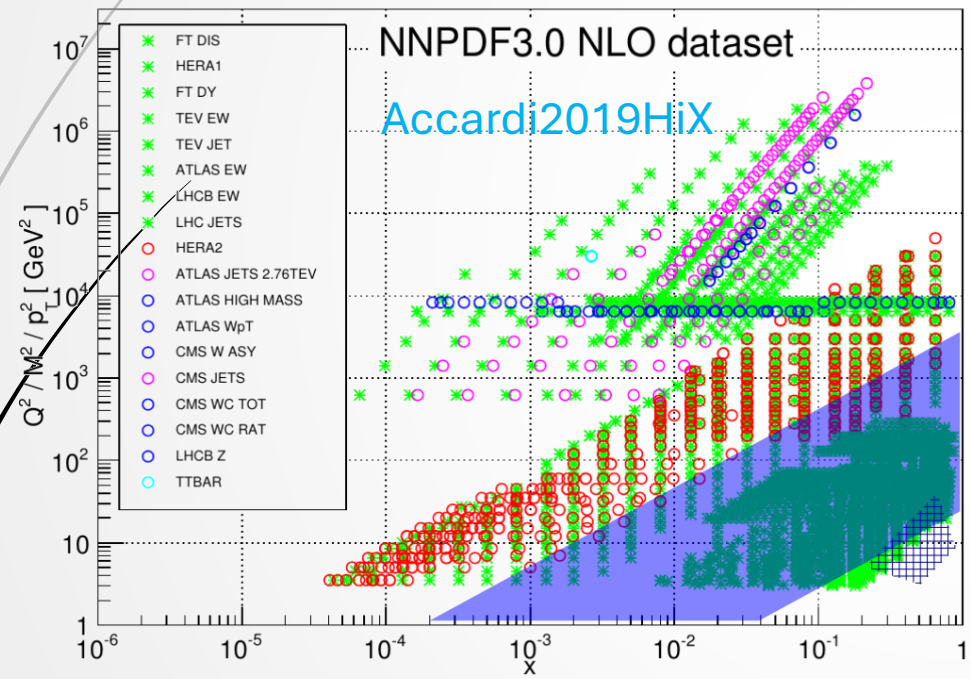

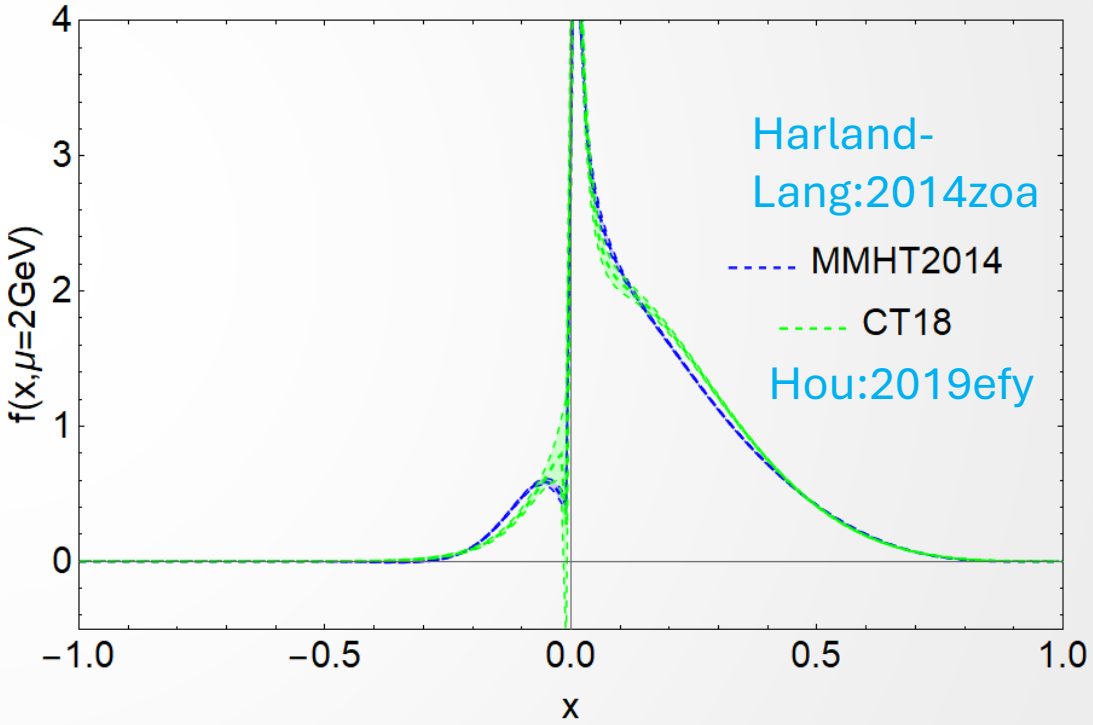

- Convenient for lattice simulation: no quark-line disconnected diagrams
- A natural benchmark to evaluate LaMET's performance on x-dependence

Previous lattice datasets

LaMET, gauge link (focus of this talk)

Works	ETMC18(Alexandrou:2018pbm) & ETMC19 (Alexandrou:2019lfo)	ETMC20 (Alexandrou:2020qtt)	LP3 (Chen:2018xof)	LPC18(LatticePartion:2018gjr)	CLQCD24(Chen:2024rgi)
Ensemble	ETMC	ETMC	MILC (a09m130)	CLS	CLQCD
a (fm)	0.0938	0.0934, 0.0820, 0.0644	0.09	0.085, 0.064	0.105
m_π (MeV)	130.4	~370	135	~350	~290, 940
P^z (GeV)	0.83, 1.11, 1.38	1.66, 1.89, 1.80	2.2, 2.6, 3.0	0~3.2	1.5~2.5

Works	JLab20(Joo:2020spy)	BNL/MSU20(Fan:2020nzz)	MSULat20(Lin:2020fsj)	ANL/BNL22(Gao:2022uhg)	ANL/BNL26(Gao:2026hix)
Ensemble	JLab/W&M	MILC (a04)	MILC	HotQCD	HotQCD
a (fm)	~0.09	0.042	0.12, 0.09, 0.06	0.076	0.0601
m_π (MeV)	358, 278, 172	310	~310, 230, 138	140	300
P^z (GeV)	Up to ~2	1.84, 2.31	up to 2.2, 2.6, 3.1	0, 0.25, 1.02, 1.53	2.43, 3.04

Pseudo PDF

LaMET, Coulomb gauge. Efforts in this direction in Qi Shi's and Joshua Lin's talks

Lattice artifacts

- The first moment calculation (zero momentum) is sensitive to excited state contaminations, discretization effects, and unphysical pion mass Mondal:2020ela

strategy	Renorm Method	$\langle x \rangle_{u-d}$ CC	CCFV
$\{4^{N\pi}, 3^*\}$	A	0.160(13)	0.145(15)
$\{4^{N\pi}, 3^*\}$	B	0.160(12)	0.145(15)
$\{4^{N\pi}, 3^*\}$	Final	0.160(13)	0.145(15)
$\{4, 3^*\}$	A	0.170(15)	0.161(16)
$\{4, 3^*\}$	B	0.168(14)	0.159(16)
$\{4, 3^*\}$	Final	0.169(15)	0.160(16)
$\{4, 2^{\text{free}}\}$	A	0.209(11)	0.193(12)
$\{4, 2^{\text{free}}\}$	B	0.206(11)	0.190(12)
$\{4, 2^{\text{free}}\}$	Final	0.208(11)	0.192(12)

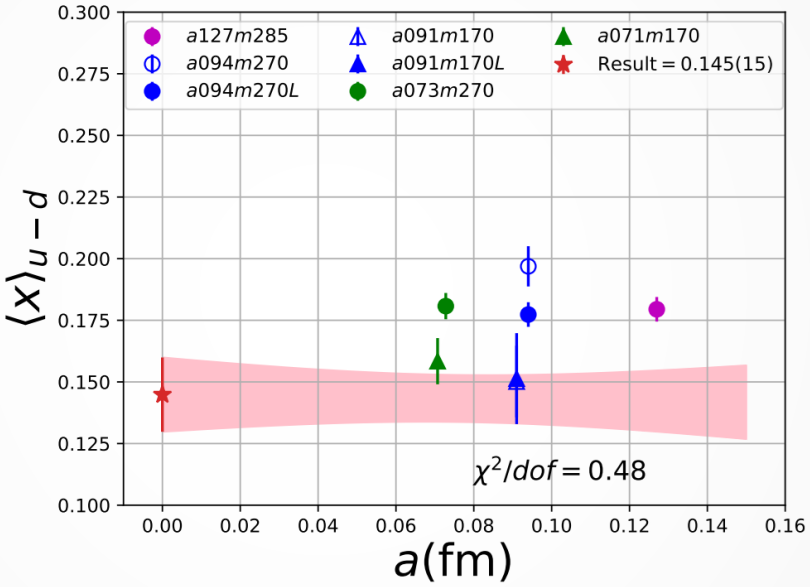

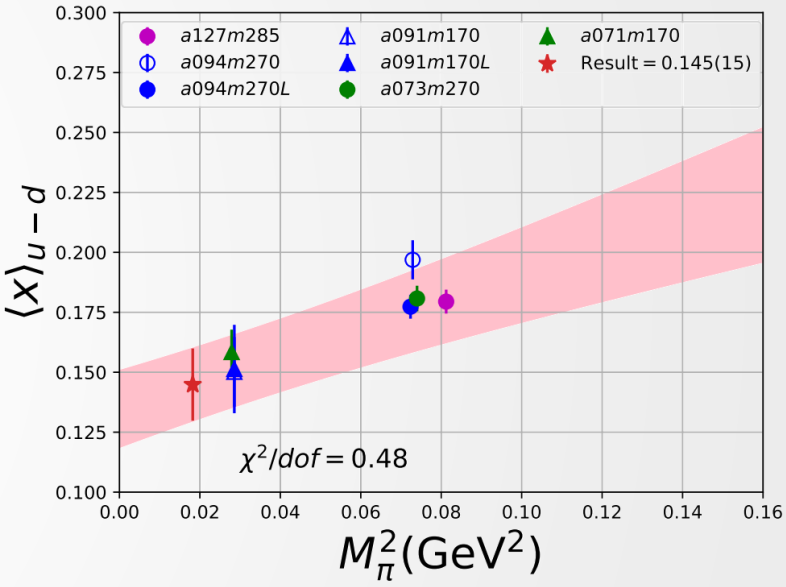

- Compared to zero momentum, these effects in large momentum matrix elements are expected to be more difficult to control.

Excited state contaminations in quasi-PDF matrix elements

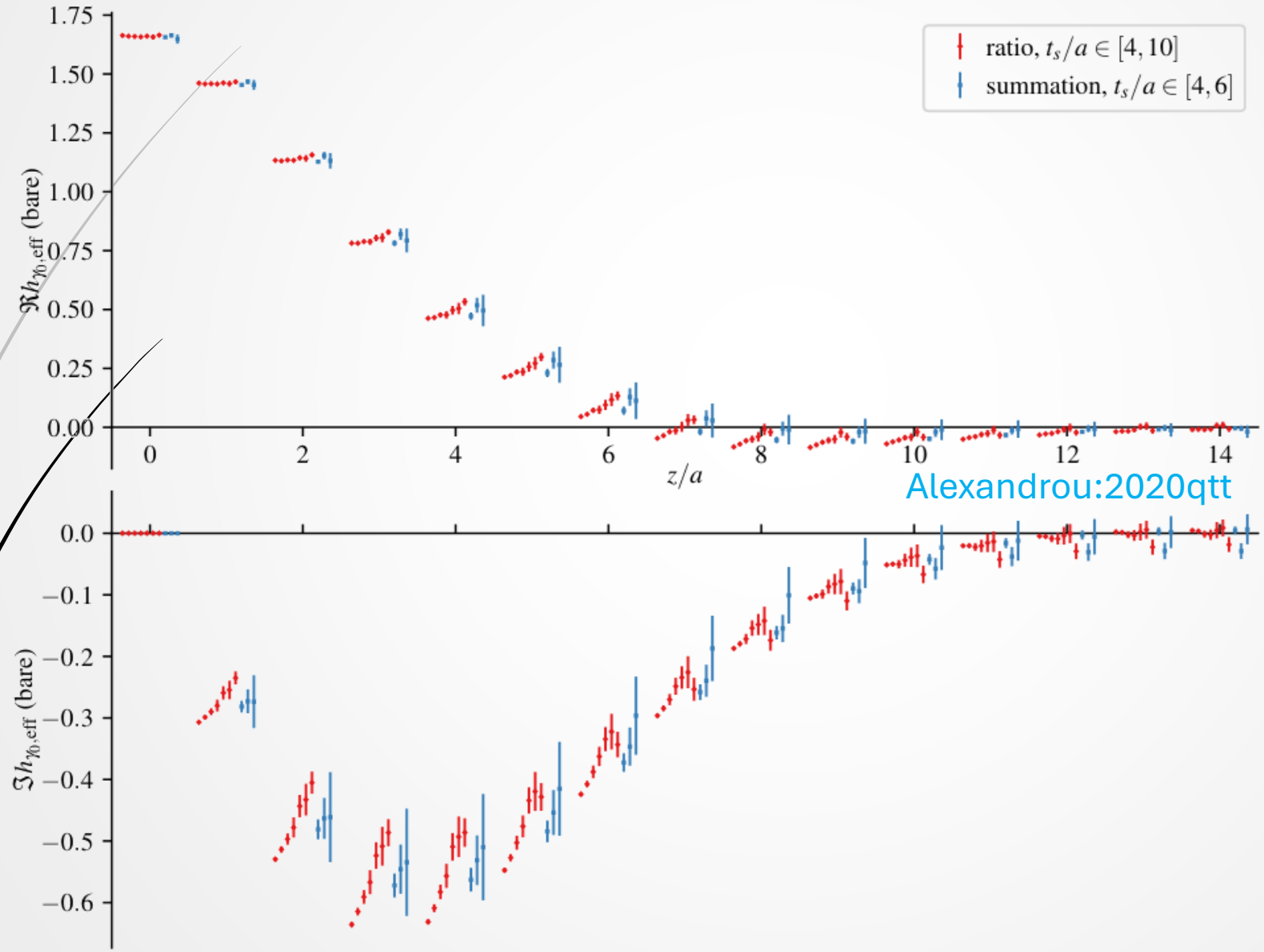

Alexandrou:2020qtt

$$h^{\mathrm{ratio}}_{\Gamma,\mathrm{eff}}(z;t_s) \equiv \frac{C^{\Gamma,z}_{3\mathrm{pt}}(\frac{t_s}{2},t_s)}{C_{2\mathrm{pt}}(t_s)} = h_\Gamma(z) + O\left(e^{-\Delta E t_s/2}\right),$$

$$h^{\mathrm{summ}}_{\Gamma,\mathrm{eff}}(z;t_s) \equiv \frac{S_{\Gamma,z}(t_s+a) - S_{\Gamma,z}(t_s)}{a} = h_\Gamma(z) + O\left(e^{-\Delta E t_s}\right),$$

$$\text{where} \quad S_{\Gamma,z}(t_s) \equiv a \sum_{\tau/a=1}^{t_s/a-1} \frac{C^{\Gamma,z}_{3\mathrm{pt}}(\tau,t_s)}{C_{2\mathrm{pt}}(t_s)}$$

Less advanced theoretical analysis

	ETMC18,19	ETMC20	LP3	LPC18
Hybrid renormalization (Ji:2020brr)	No	No	No	No
Latest large distance formulas (Ji:2026vir)	No	No	No	No
Perturbative resummations (Gao:2021hxl,Su:2022fiu,Zhang:2023bxs,Ji:2023pba,Liu:2023onm,Ji:2024hit)	No	No	No	No
	CLQCD24	**BNL/MSU20**	**MSULat20**	**ANL/BNL22**
Hybrid renormalization	Yes	No	No	Yes
Latest large distance formulas	No	No	No	No
Perturbative resummations	RGR+LRR No TR	No	No	No

Various shapes in x-space

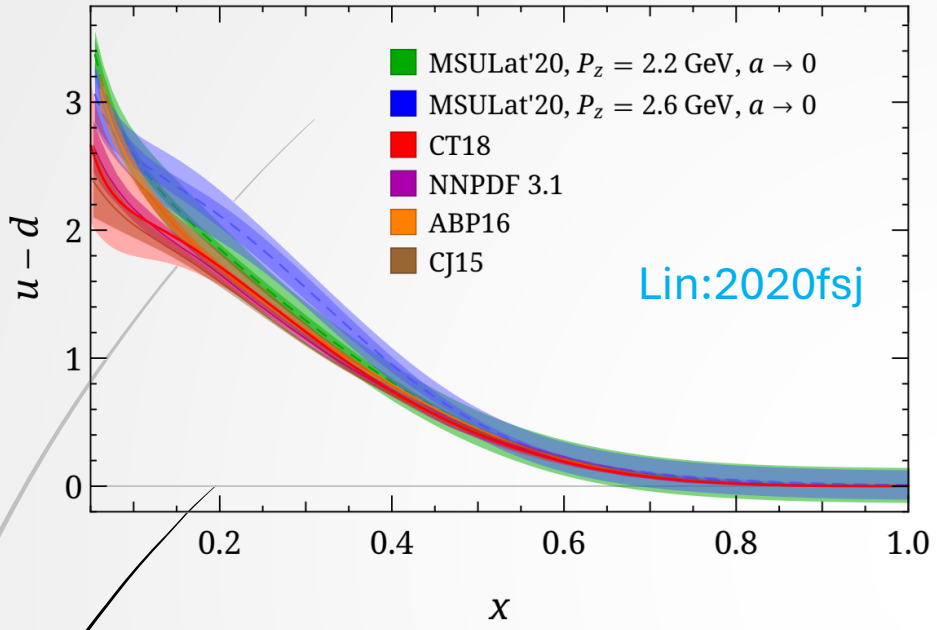

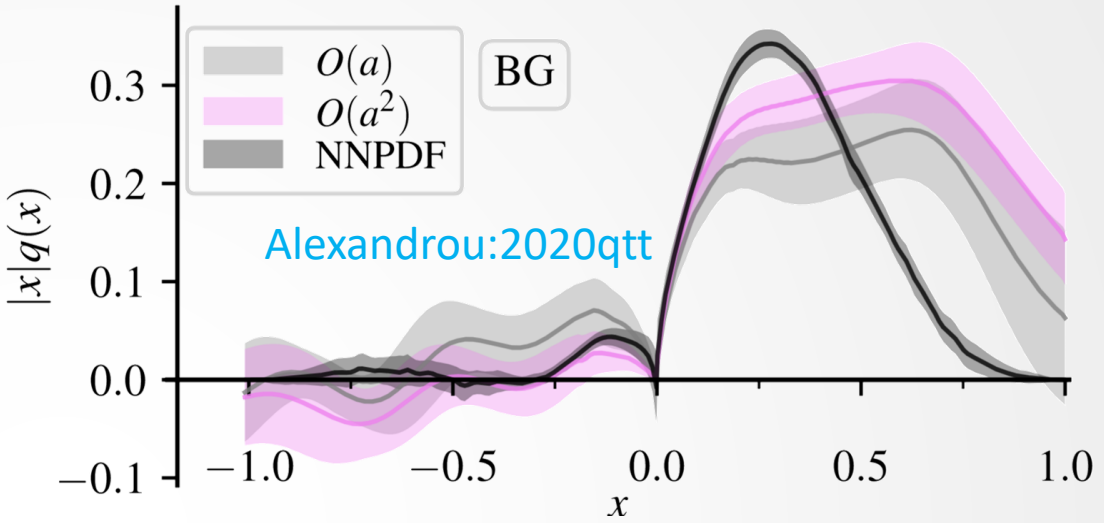

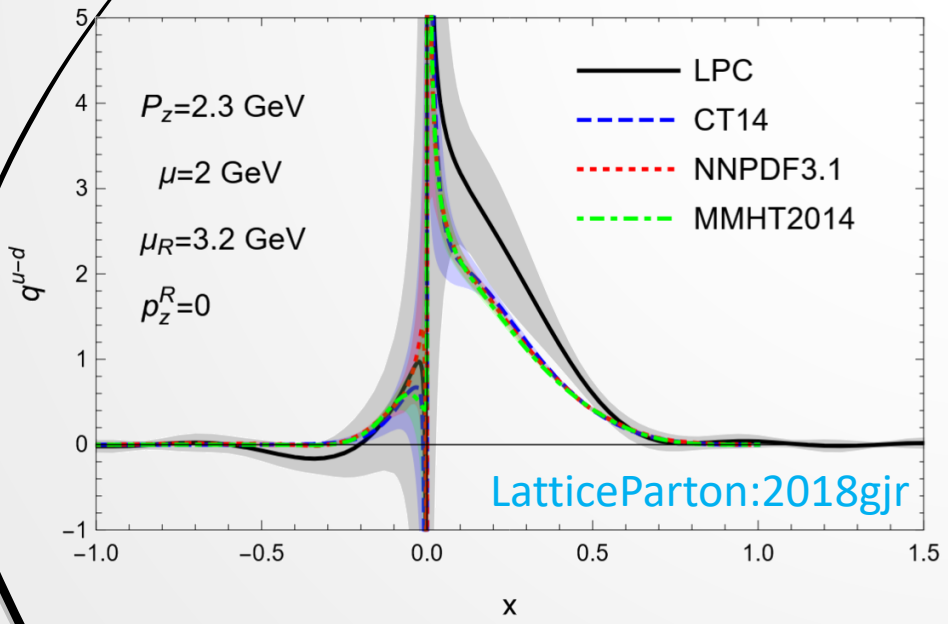

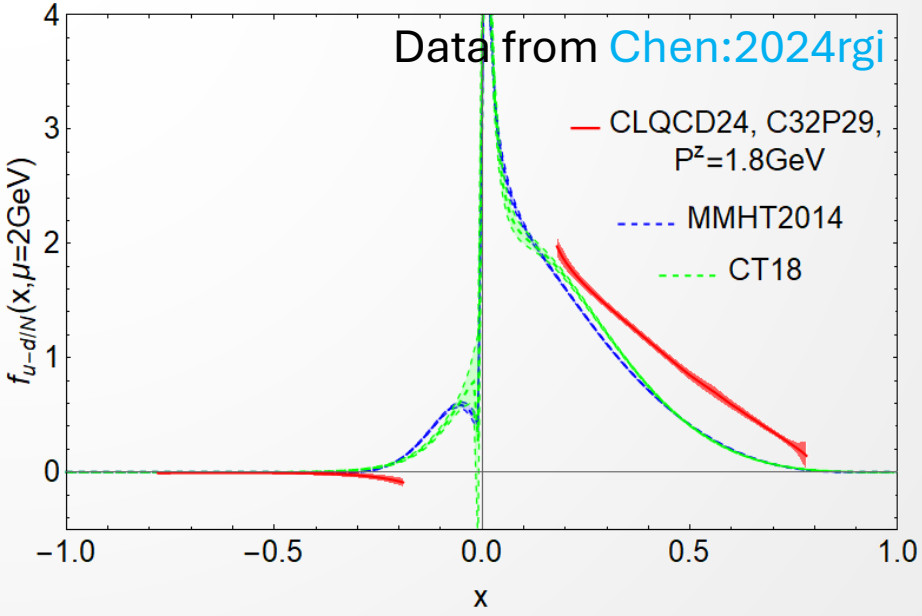

Outline

Benchmark of LaMET	Proton unpolarized isovector PDF as a benchmark to evaluate LaMET's x-dependence calculation; Previous works: lattice artifacts and less-advanced theoretical analysis lead to inconsistent results among lattice groups and many deviate from phenomenological PDFs.
Reanalysis of lattice datasets	Incorporating all the latest theoretical tools; Mitigating lattice artifacts empirically.
LaMET results compared with global fit	The variations among lattice groups are dramatically reduced; The physical-limit result is consistent with global fit PDF within $\sim 1\sigma$.

Selected datasets

Works	MSULat20(Lin:2020fsj)	ETMC20 (Alexandrou:2020qtt)	LPC18(LatticeParton:2018gjr)	CLQCD24(Chen:2024rgi)
Ensemble	MILC	ETMC (B55)	CLS	CLQCD
a (fm)	0.12, 0.09, 0.06	0.0820	0.085	0.105
m_π (MeV)	~310, 230, 138	~370	350	~290
P^z (GeV)	2.2	1.89	2.3	1.85

They are selected under the following considerations:

- large momentum (at least $\sim 2\mathrm{GeV}$, corresponding to $v \sim 0.9c$);
- statistical precision;
- data accessibility.

Hybrid renormalization Ji:2020brr

- Basic idea: an almost minimal UV subtraction while mitigating short-distance discrepancies between lattice and continuum theories.
- Formulation:

$$\tilde{h}^R(z,P^z) = \frac{\tilde{h}^B(z,P^z,a)}{\tilde{h}^B(z,0,a)}\theta[z_s-|z|] + \frac{\tilde{h}^B(z,P^z,a)}{Z_R(z,\mu,a)}\frac{Z_R(z_s,\mu,a)}{\tilde{h}^B(z_s,0,a)}\theta[|z|-z_s]$$

where $Z_R(z,\mu,a)$ is determined using the methods in LatticePartonLPC:2021gpi and Zhang:2023bxs using NNLO+RGR+LRR pert.

- Hybrid renormalized matrix elements:

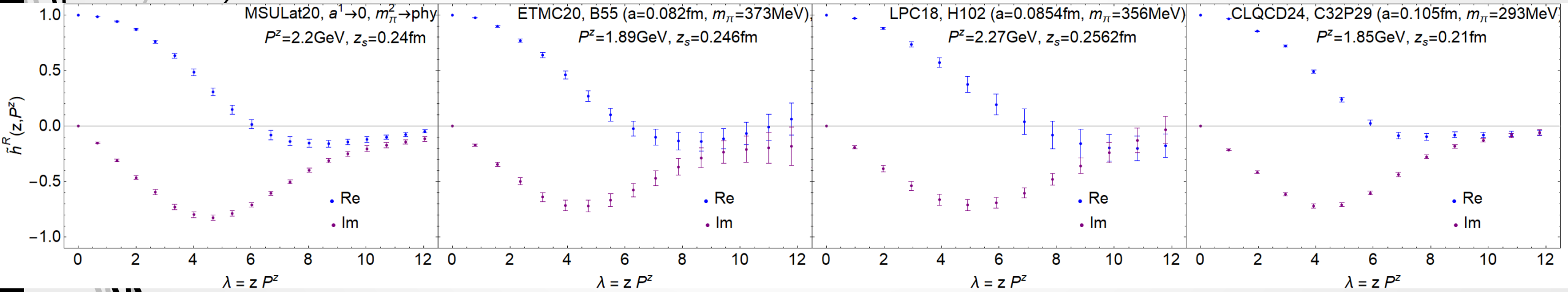

Mitigating lattice artifacts

- Idea: enforce the first moment $\langle x \rangle$ of lattice data to match the phenomenological result.
- A mitigation formula should impact short distance slope of imaginary part: $1 + i\ z\ P^z \delta y$. To avoid unrealistically large imaginary part at large z, we unitarize it to an exponential:

$$\tilde{h}(z, P^z) = \tilde{h}^R(z, P^z) e^{i\ z\ P^z \delta y}$$

where δy is determined by fitting the imaginary part of $\tilde{h}(z, P^z)$ to the short distance OPE

$$1 - i\ z\ P^z\ \langle x \rangle(\mu)\ \frac{C_1(z^2\mu^2)}{C_0(z^2\mu^2)} + \cdots$$

where the first moment is fixed to CT18 value $\langle x \rangle(\mu = 2\text{GeV}) = 0.1562(24)$, and the Wilson coefficients C_i are NNLO+RGR+LRR accuracy.

- Results

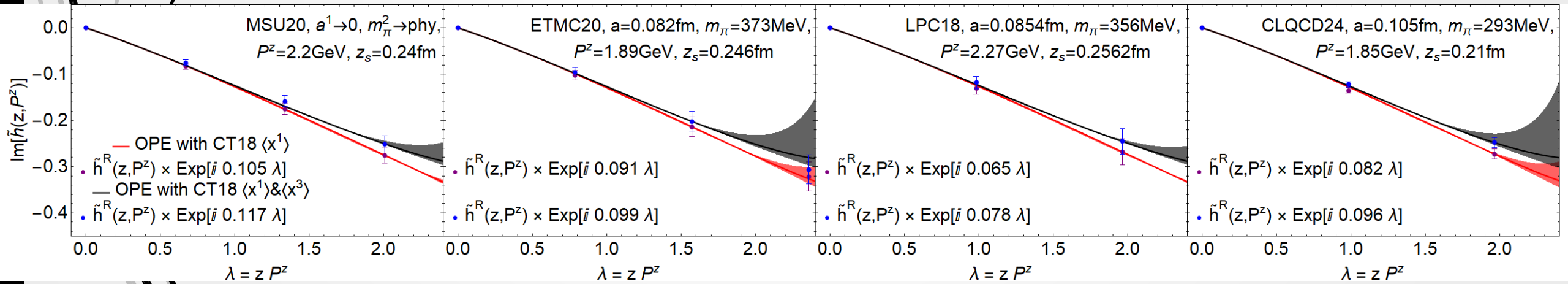

Large distance extrapolation and Fourier transform

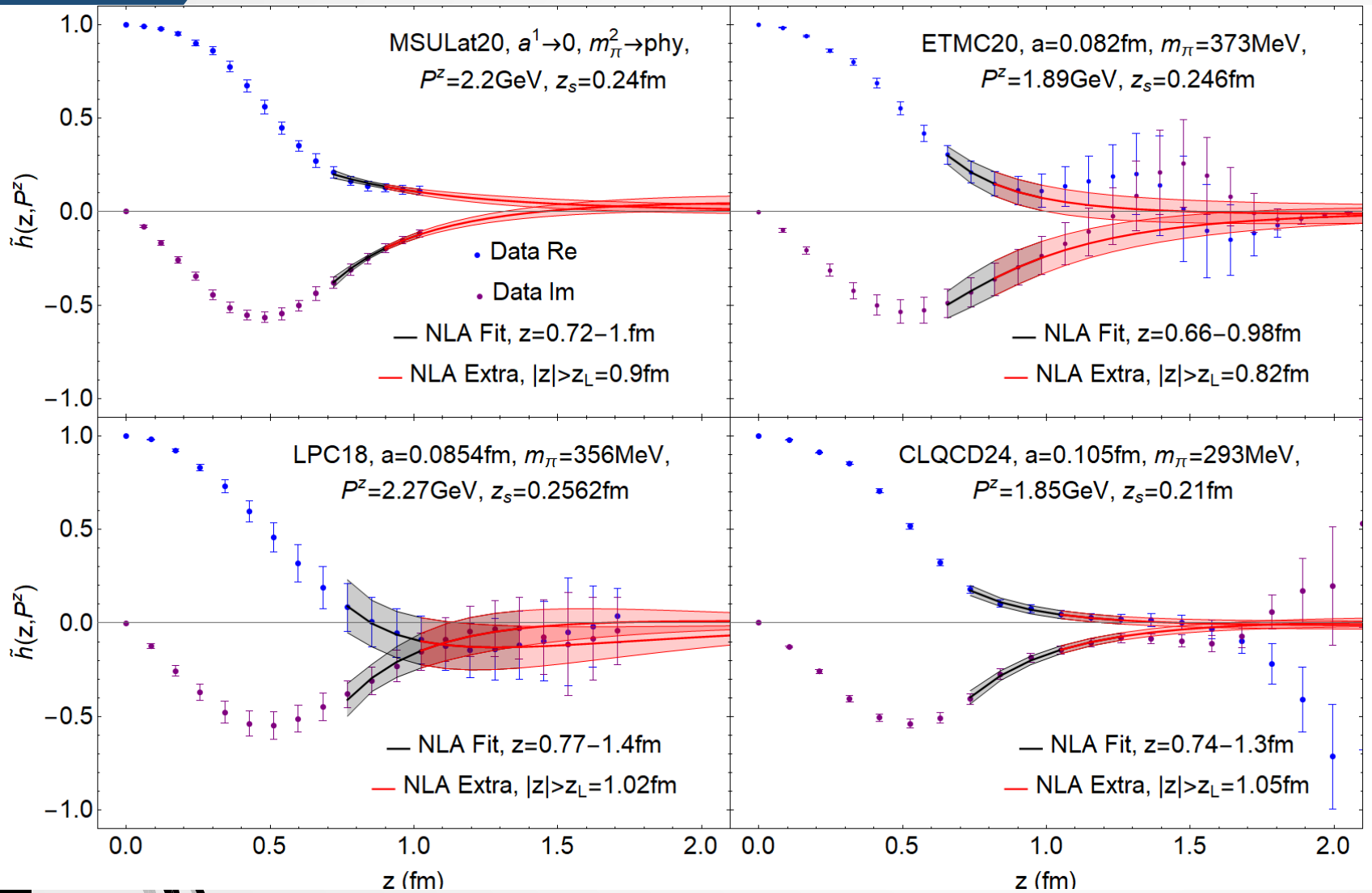

- Use large distance asymptotic formulas (Ji:2026vir) as physical constraints:

$$\tilde{h}^{\text{asym}}(z,P^z) = \left[A e^{i\,\phi\,\text{sgn}(z)} + \frac{A' e^{i\,\phi'\,\text{sgn}(z)}}{|z|}\right] e^{-\Lambda\,|z|}$$

- Fourier transform

$$\tilde{f}(y,P^z) = P^z \int \frac{dz}{2\pi} e^{i\,z\,P^z\,y}\left[\tilde{h}(z,P^z)\theta(z_L-|z|) + \tilde{h}^{\text{asym}}(z,P^z)\theta(|z|-z_L)\right]$$

Perturbative matching

- Purpose: deal with the UV difference between PDF and LMD (Xiong:2013bka,Ma:2014jla,Ma:2017pxb,Izubuchi:2018srq,Wang:2019tgg,Ji:2020ect):

$$f(x,\mu) = \int \frac{dy}{|y|} C\left(\frac{x}{y}, \frac{\mu}{|y|P^z}\right) \tilde{f}(y, P^z) + O\left(\frac{\Lambda_{\mathrm{QCD}}^2}{x^2 P_z^2}, \frac{\Lambda_{\mathrm{QCD}}^2}{(1-x)^2 P_z^2}\right)$$

- The matching kernel $C\left(\frac{x}{y}, \frac{\mu}{|y|P^z}\right)$ is at NNLO+RGR+LRR+TR accuracy:
  - Next-to-next-to-leading order (NNLO) (Li:2020xml,Chen:2020ody): perturbative precision
  - DGLAP log resummation (RGR) (Su:2022fiu): precision control at small x
  - Threshold log resummation (TR) (Gao:2021hxl,Ji:2023pba,Liu:2023onm,Ji:2024hit): precision control at large x
  - Leading renormalon resummation (LRR) (Zhang:2023bxs): perturbative convergence, linear power accuracy

Outline

Benchmark of LaMET

Proton unpolarized isovector PDF as a benchmark to evaluate LaMET's x-dependence calculation;
Previous works: lattice artifacts and less-advanced theoretical analysis lead to inconsistent results among lattice groups and many deviate from phenomenological PDFs.

Reanalysis of lattice datasets

Incorporate [illegible] theoretical tools;
Mitigate [illegible] systematically.

LaMET results compared with global fit

The variations among lattice groups are dramatically reduced;
The physical-limit result is consistent with global fit PDF within $\sim 1\sigma$.

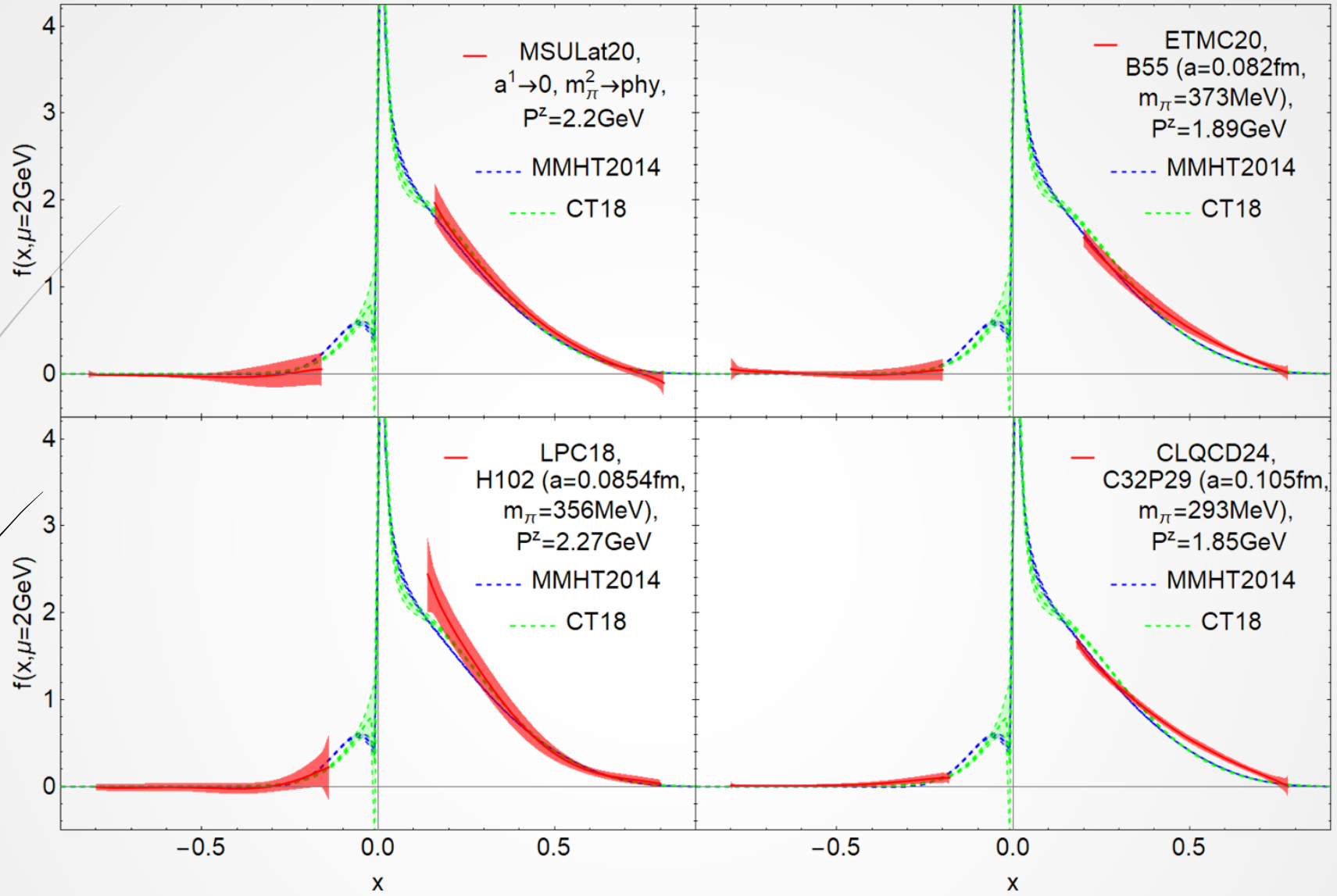

- After implementing a unified analysis framework, the spread among the resulting PDFs is substantially reduced compared with the original analyses.
- The physical-limit lattice PDF is consistent with phenomenological PDFs within $\sim 1\sigma$. The remaining datasets exhibit broadly compatible x-dependence.

Conclusions

- We present a LaMET calculation of the proton isovector unpolarized PDF using existing lattice QCD datasets, along with theoretical precision-control techniques and an empirical method to remove a large part of lattice artifacts.
- The disagreement among earlier lattice PDF calculations appears to be largely attributable to analysis methodology and lattice artifacts.
- The resulting PDFs align with phenomenological determinations, supporting LaMET's potential to achieve quantitatively reliable determinations of the x-dependence of parton distributions.

Appendix

Evidence of excited state contamination

$$h^{\text{ratio}}_{\Gamma,\text{eff}}(z;t_s) \equiv \frac{C^{\Gamma,z}_{\text{3pt}}(\frac{t_s}{2},t_s)}{C_{\text{2pt}}(t_s)} = h_\Gamma(z) + O\left(e^{-\Delta E t_s/2}\right),$$

$$h^{\text{summ}}_{\Gamma,\text{eff}}(z;t_s) \equiv \frac{S_{\Gamma,z}(t_s+a) - S_{\Gamma,z}(t_s)}{a} = h_\Gamma(z) + O\left(e^{-\Delta E t_s}\right),$$

$$\text{where} \quad S_{\Gamma,z}(t_s) \equiv a \sum_{\tau/a=1}^{t_s/a-1} \frac{C^{\Gamma,z}_{\text{3pt}}(\tau,t_s)}{C_{\text{2pt}}(t_s)}$$

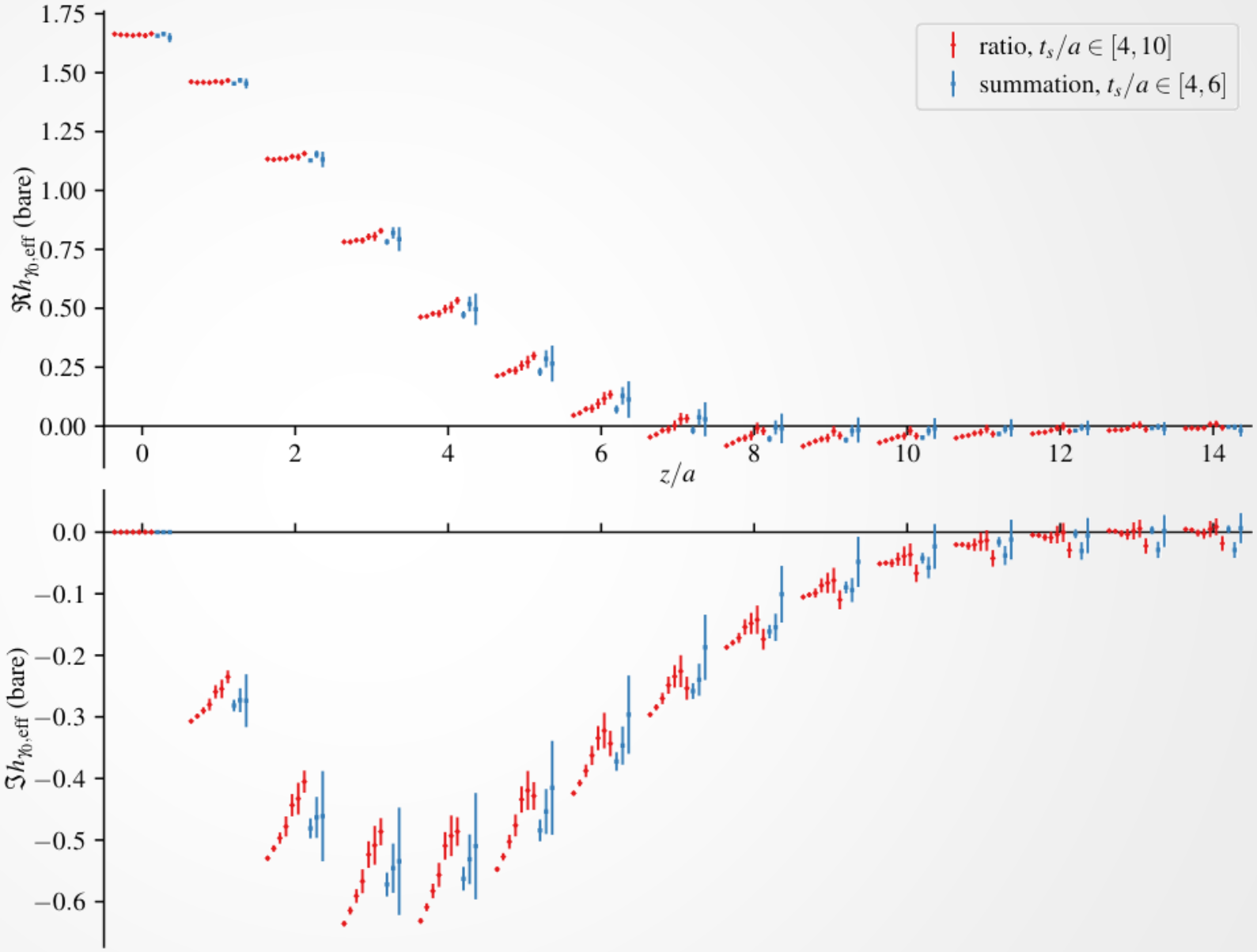

Alexandrou:2020qtt

Evidence of excited state contamination

$$R\left[t_{sep}, t=\frac{t_{\mathrm{sep}}}{2}\right]=\frac{\mathrm{C}_3[t_{\mathrm{sep}},\ t=\frac{t_{\mathrm{sep}}}{2},\ z,\ P_z]}{C_2[t_{\mathrm{sep}},\ P_z]}$$

$$S[t_{\mathrm{sep}},\tau_c]=\sum_{t=\tau_c}^{t_{sep}-\tau_c} R[t_{sep},t]$$

$$FH[t_{\mathrm{sep}},\tau_c]=S[t_{\mathrm{sep}}+1,\tau_c]-S[t_{\mathrm{sep}},\tau_c]$$

$$\tau_c=2$$

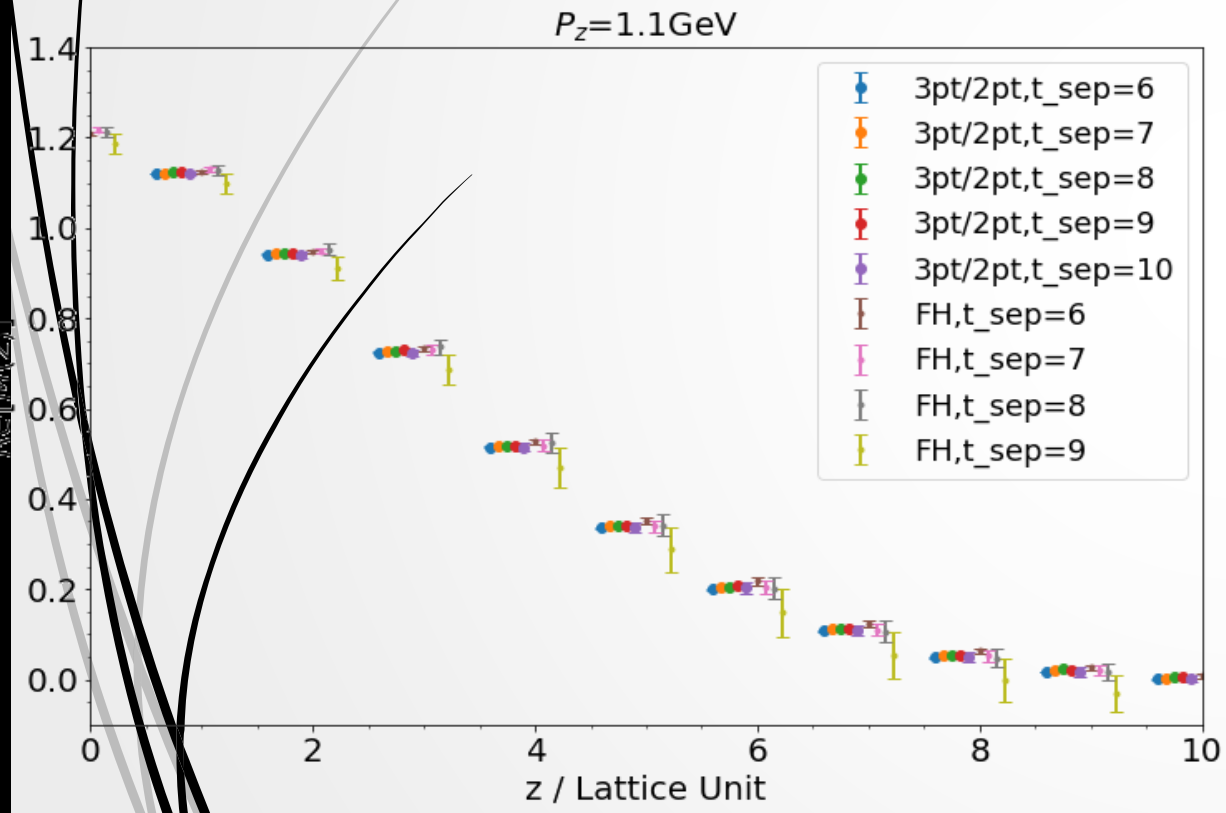

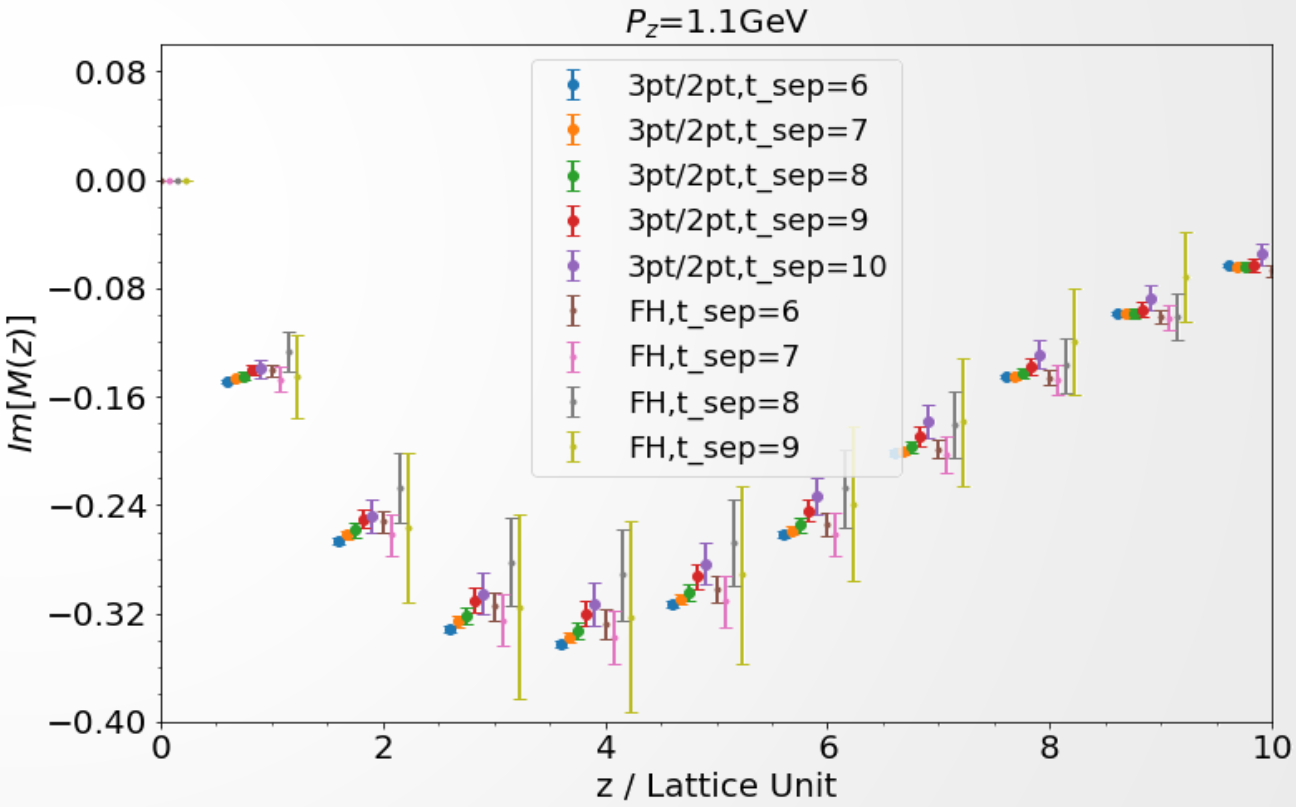

Data from Chen:2024rgi

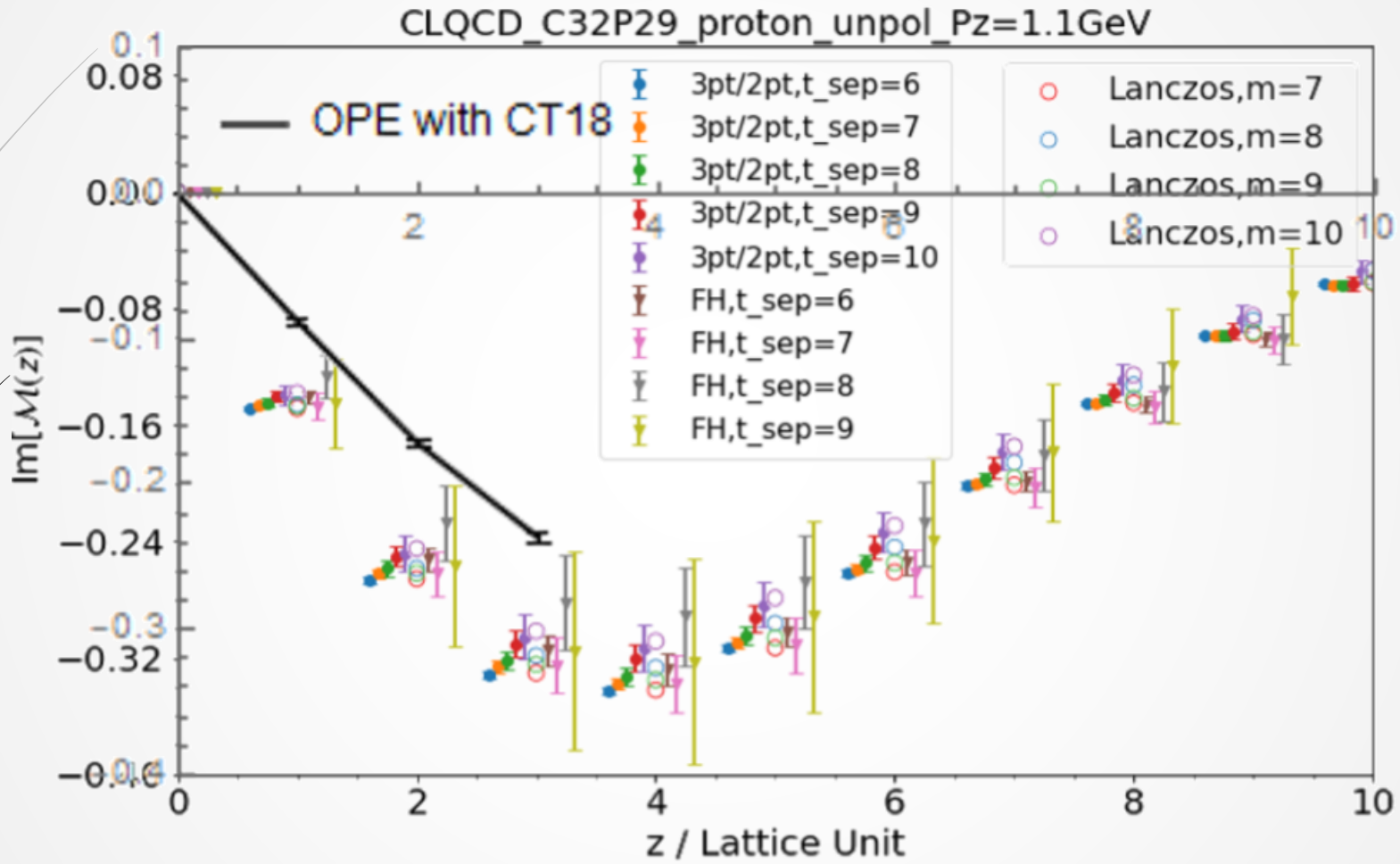
CLQCD_C32P29_proton_unpol_Pz=1.1GeV
OPE with CT18
3pt/2pt,t_sep=6
3pt/2pt,t_sep=7
3pt/2pt,t_sep=8
3pt/2pt,t_sep=9
3pt/2pt,t_sep=10
FH,t_sep=6
FH,t_sep=7
FH,t_sep=8
FH,t_sep=9
Lanczos,m=7
Lanczos,m=8
Lanczos,m=9
Lanczos,m=10
Im[ℳ(z)]
z / Lattice Unit

Reanalysis of selected datasets

Works	ETMC18(Alexandrou:2018pbm) & ETMC19 (Alexandrou:2019lfo)	ETMC20 (Alexandrou:2020qtt)	LP3 (Chen:2018xof)	LPC18(LatticeParton:2018gjr)	CLQCD24(Chen:2024rgi)
Ensemble	ETMC	ETMC (B55)	MILC (a09m130)	CLS	CLQCD
a (fm)	0.0938	0.0820	0.09	0.085	0.105
m_π (MeV)	130.4	~370	135	350	~290
P^z (GeV)	0.83, 1.11, 1.38	1.89	2.2, 2.6, 3.0	2.3	1.85

Works	BNL/MSU20(Fan:2020nzz)	MSU20(Lin:2020fsj)	ANL/BNL22(Gao:2022uhg)
Ensemble	MILC (a04)	MILC	HotQCD
a (fm)	0.042	0.12, 0.09, 0.06	0.076
m_π (MeV)	310	~310, 230, 138	140
P^z (GeV)	1.84, 2.31	2.2	0, 0.25, 1.02, 1.53

LaMET analysis procedure

- Lattice data generation of $(u-d)/N$ quasi-PDF matrix element

$$\tilde{h}^B(z,P^z,a) = \langle N(P^z)| \left[\bar{u}(z)\gamma^t U(z,0)u(0) - \bar{d}(z)\gamma^t U(z,0)d(0)\right] |N(P^z)\rangle$$

- Hybrid renormalization

$$\tilde{h}^R(z,P^z) = \frac{\tilde{h}^B(z,P^z,a)}{\tilde{h}^B(z,0,a)}\theta[z_s-|z|] + \frac{\tilde{h}^B(z,P^z,a)}{Z_R(z,\mu,a)}\frac{Z_R(z_s,\mu,a)}{\tilde{h}^B(z_s,0,a)}\theta[|z|-z_s]$$

where $Z_R(z,\mu,a)$ is determined using the methods in LatticePartonLPC:2021gpi and Zhang:2023bxs using NNLO+RGR+LRR pert.

- Calibration of first moment

$$\tilde{h}(z,P^z) = \tilde{h}^R(z,P^z)e^{i\,z\,P^z\,\Gamma}$$

where Γ is determined by fitting imaginary part of $\tilde{h}(z,P^z)$ at $|z|<z_s$ to the short distance OPE with $\langle x\rangle$:

$$\tilde{h}(z,P^z) = 1 - i\,z\,P^z\,\langle x\rangle(\mu)\,\frac{C_1(z^2\mu^2)}{C_0(z^2\mu^2)} + \cdots$$

where $C_\#$ are NNLO+RGR+LRR Wilson coefficients.

- Large distance asymptotic analysis. Fit and extrapolate $\tilde{h}(z,P^z)$ to large distance based on Ji:2026vir. Then perform the Fourier transformation:

$$\tilde{f}(y,P^z) = P^z\int\frac{dz}{2\pi}e^{i\,z\,P^z y}\tilde{h}(z,P^z)$$

- Perturbative matching

$$f(x,\mu) = \int\frac{dy}{|y|}C\left(\frac{x}{y},\frac{\mu}{y\,P^z}\right)\tilde{f}(y,P^z)$$

where $C\left(\frac{x}{y},\frac{\mu}{y\,P^z}\right)$ is the NNLO+RGR+LRR+TR matching kernel in Ji:2024hit. All the LRRs mentioned here are in the same renormalon scheme.

MSU20(Lin:2020fsj) – Conversion to hybrid scheme

- Fig.~4 of Lin:2020fsj shows the RIMOM renormalized matrix element

$$\tilde{h}^{\mathrm{RM}}(z,P^z)=\frac{\tilde{h}^{B}(z,P^z,a)}{Z^{\mathrm{RM}}(z,a)}$$

to implement LaMET analysis, we need to convert it to hybrid scheme

- According to LatticePartonLPC:2021gpi, the RM factor can be factorized into the renormalization factor and intrinsic nonperturbative physics

$$Z^{\mathrm{RM}}(z,a)=Z_R(z,\mu,a)Z^{\mathrm{RM-inp}}(z,\mu)$$

So does the zero momentum matrix element

$$\tilde{h}^{B}(z,0,a)=Z_R(z,\mu,a)\tilde{h}^{B-\mathrm{inp}}(z,\mu)$$

Therefore, the conversion can be implemented as follows

$$\tilde{h}^{R}(z,P^z)=\frac{\tilde{h}^{\mathrm{RM}}(z,P^z)Z^{\mathrm{RM}}(z,a)}{\tilde{h}^{B}(z,0,a)}\theta[z_s-|z|]+\frac{\tilde{h}^{\mathrm{RM}}(z,P^z)Z^{\mathrm{RM}}(z,a)}{Z_R(z,\mu,a)}\frac{Z_R(z_s,\mu,a)}{\tilde{h}^{B}(z_s,0,a)}\theta[|z|-z_s]$$

$$=\frac{\tilde{h}^{\mathrm{RM}}(z,P^z)Z^{\mathrm{RM-inp}}(z,\mu)}{\tilde{h}^{B-\mathrm{inp}}(z,\mu)}\theta[z_s-|z|]+\frac{\tilde{h}^{\mathrm{RM}}(z,P^z)Z^{\mathrm{RM-inp}}(z,\mu)}{\tilde{h}^{B-\mathrm{inp}}(z_s,\mu)}\theta[|z|-z_s]$$

- In practice, $\tilde{h}^{\mathrm{RM}}(z,P^z)$ is digitized from Fig.~4 of Lin:2020fsj, $Z^{\mathrm{RM}}(z,a)$ from Fig.~2 of Lin:2020fsj, and $\tilde{h}^{B}(z,0,a)$ from LatticePartonLPC:2021gpi. The $Z^{\mathrm{RM-inp}}(z,\mu)$ and $\tilde{h}^{B-\mathrm{inp}}(z,\mu)$ are extracted from $Z^{\mathrm{RM}}(z,a)$ and $\tilde{h}^{B}(z,0,a)$ following the methods in LatticePartonLPC:2021gpi and Zhang:2023bxs.

Impacts of renormalization methods

- Different renormalization methods using LPC18 dataset

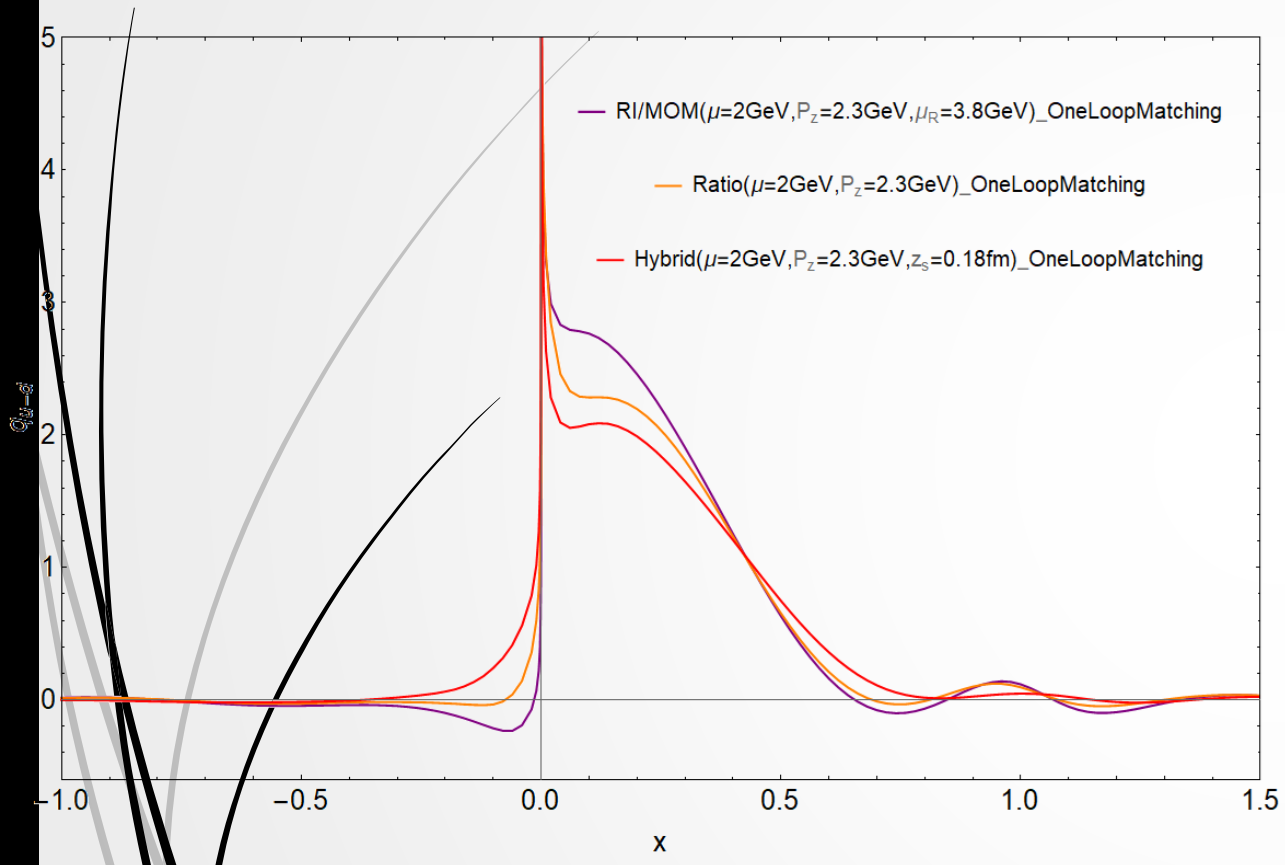

- Influence from m_0

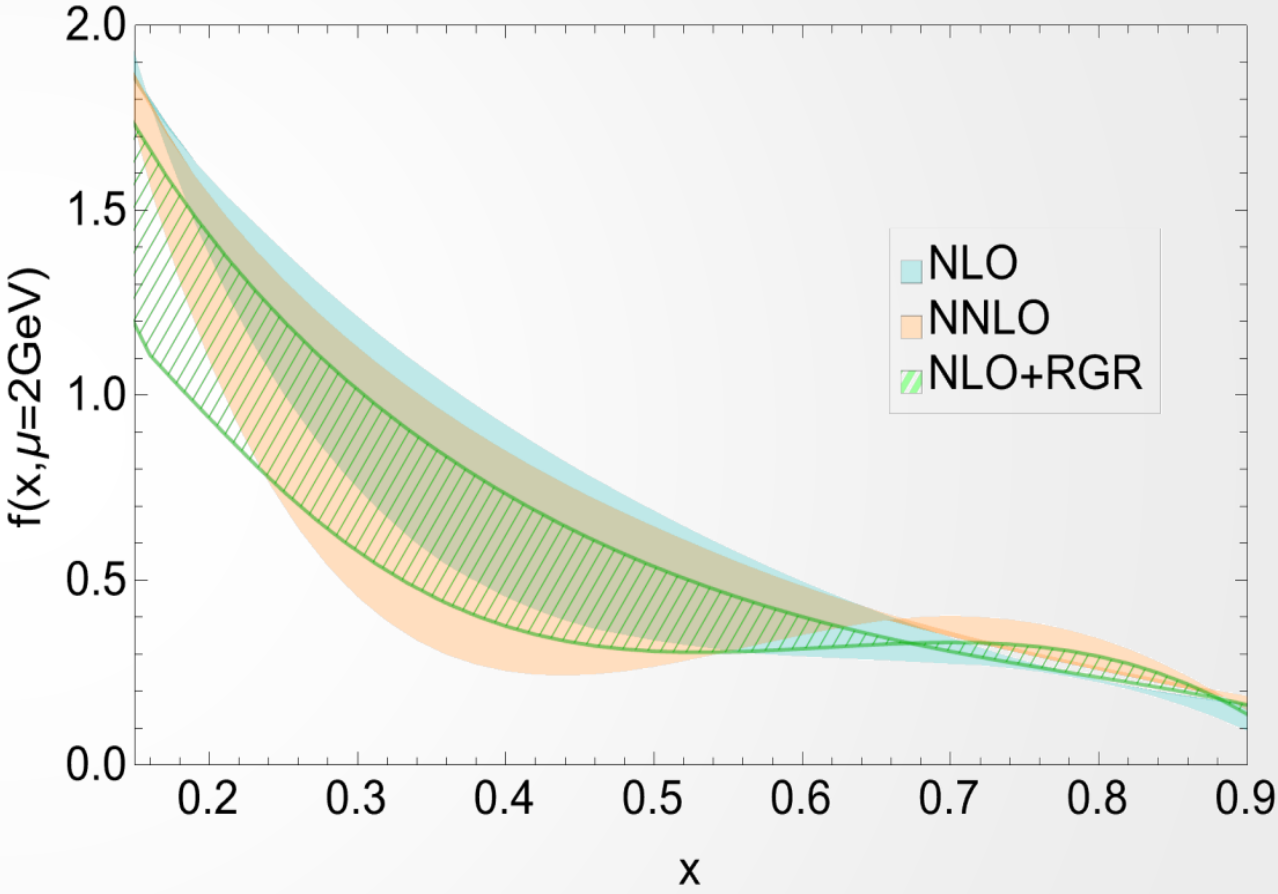

Zhang:2023bxs

Test on z_s

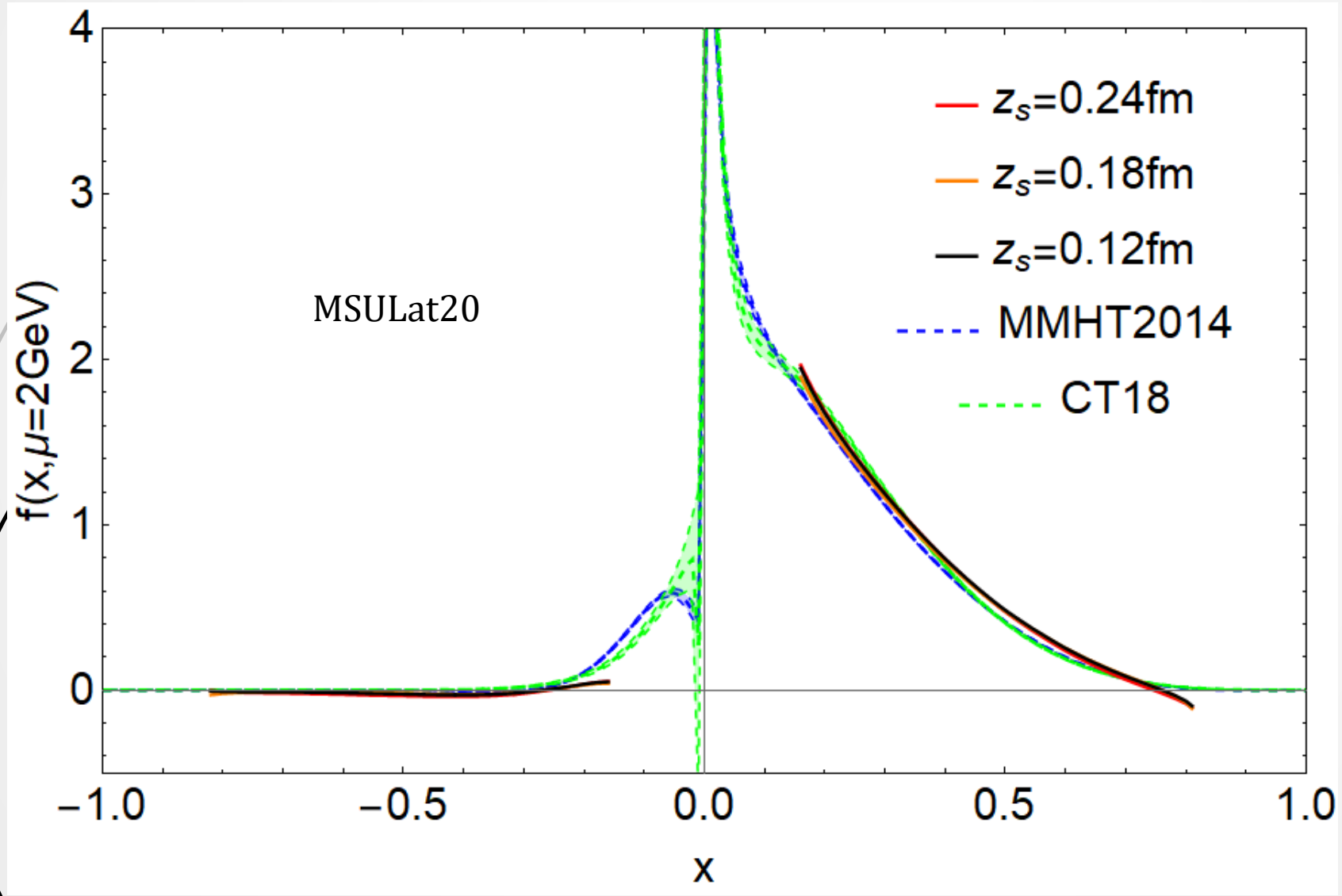
MSULat20
z_s=0.24fm
z_s=0.18fm
z_s=0.12fm
MMHT2014
CT18
f(x,μ=2GeV)
x
4
3
2
1
0
−1.0
−0.5
0.0
0.5
1.0

Without and with the calibration of $\langle x \rangle$

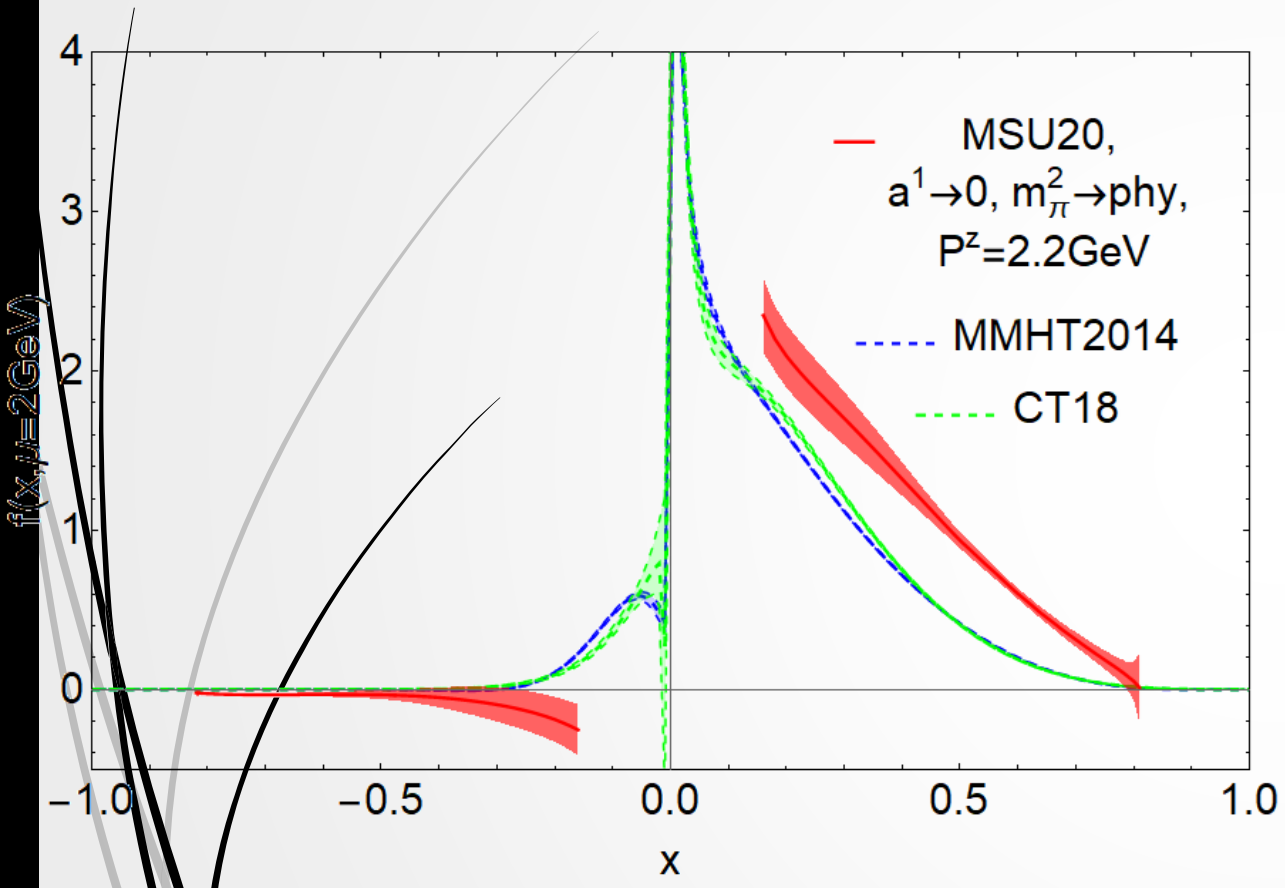

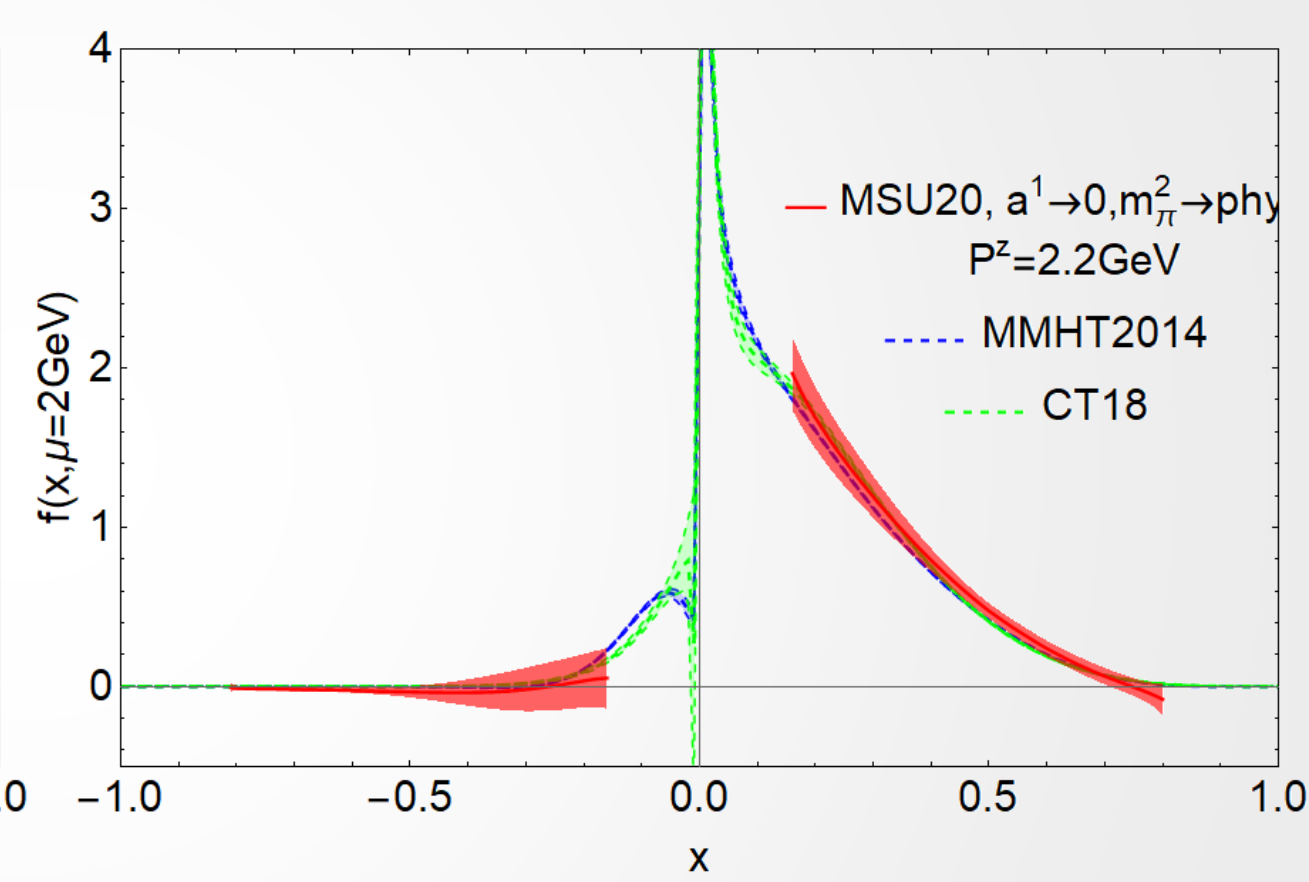

Without the calibration of $\langle x \rangle$

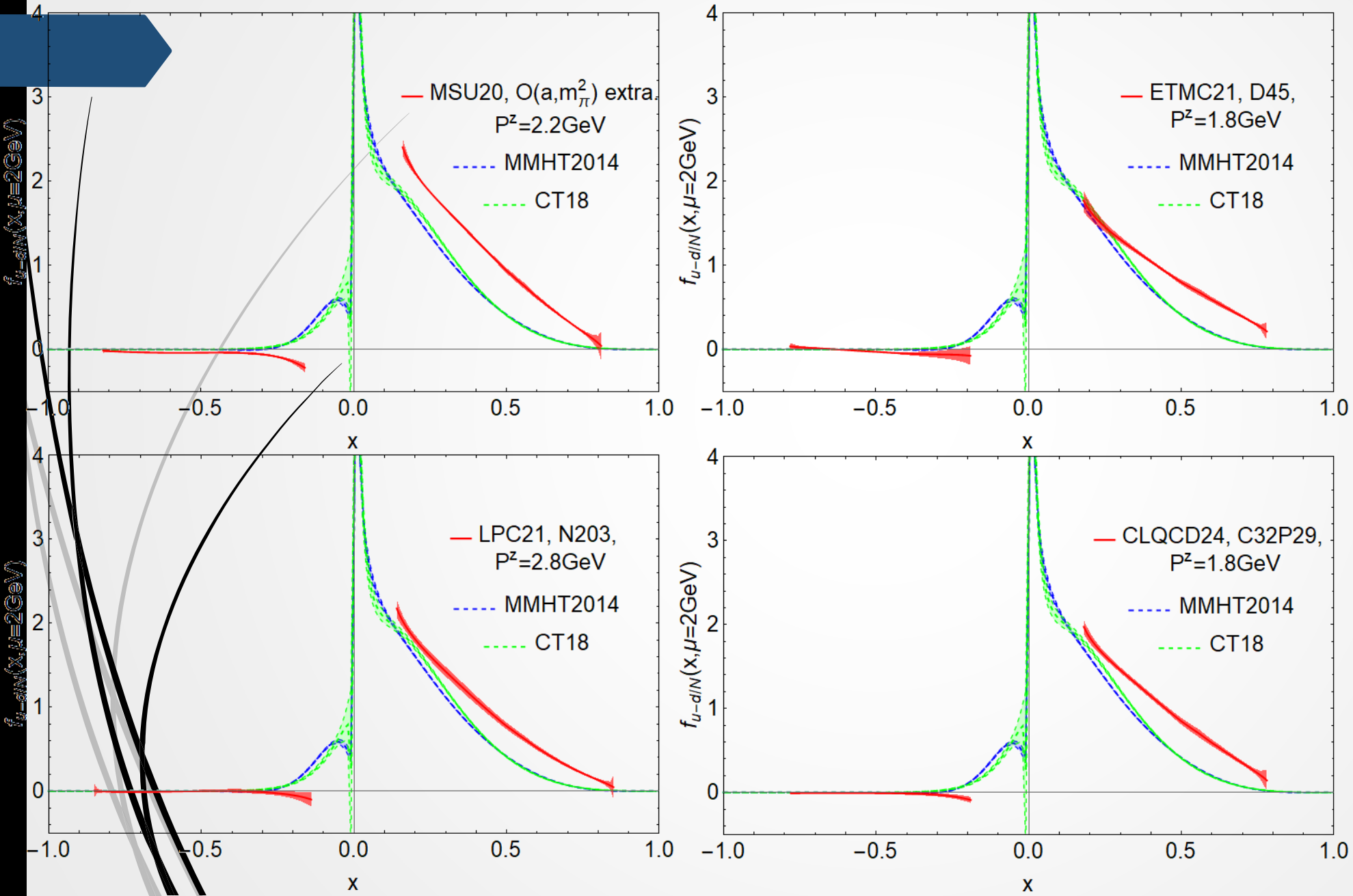

- Without any modifications, the lattice PDFs deviate a lot from global fit ones.
- CLQCD and LPC contain stat err. MSU20 and ETMC21 do not.

Comparing calibration ansatz

$$\tilde{h}(z, P^z) = \tilde{h}^R(z, P^z) e^{i\, z\, P^z \delta y}$$

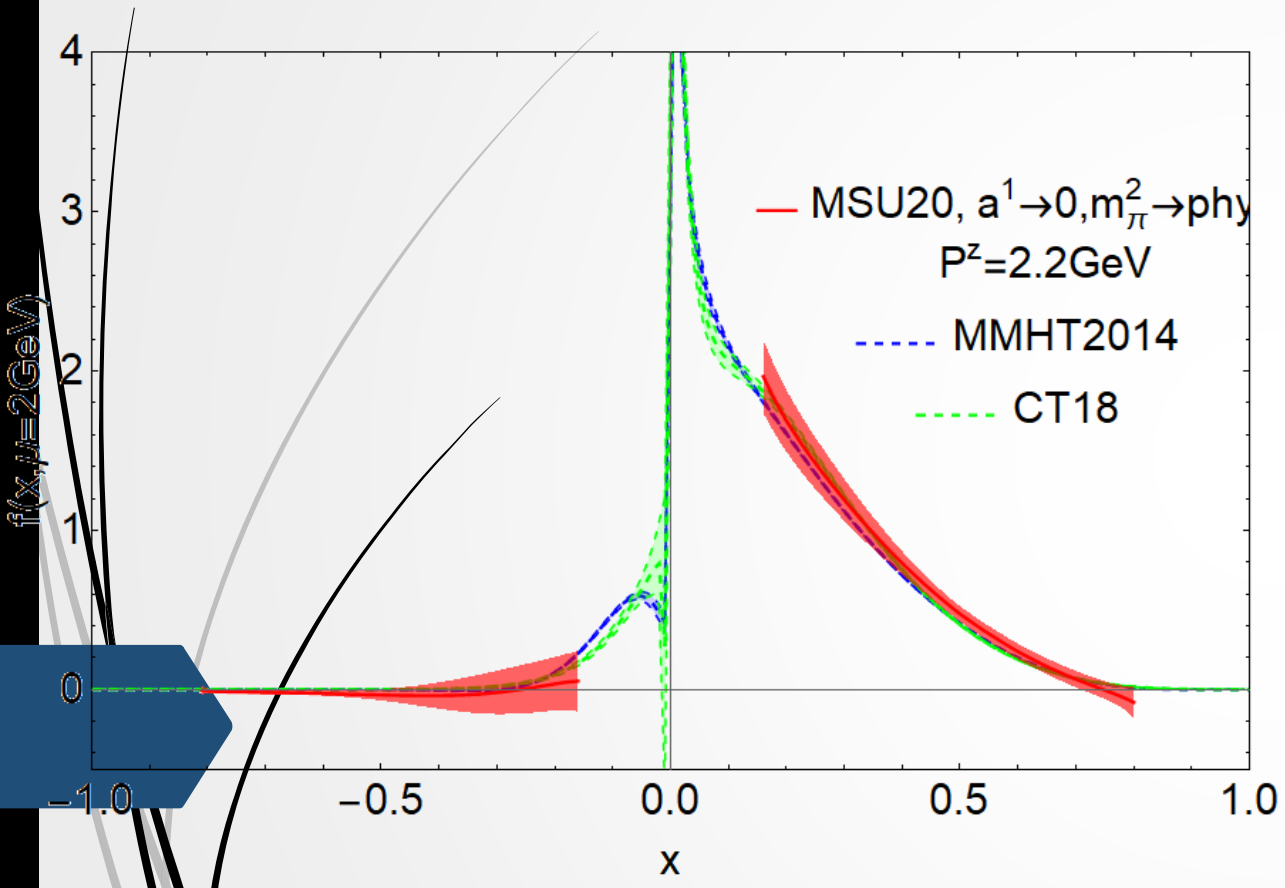

$$\tilde{h}(z, P^z) = \tilde{h}^R(z, P^z)(1 + i\, z\, P^z \delta y)$$

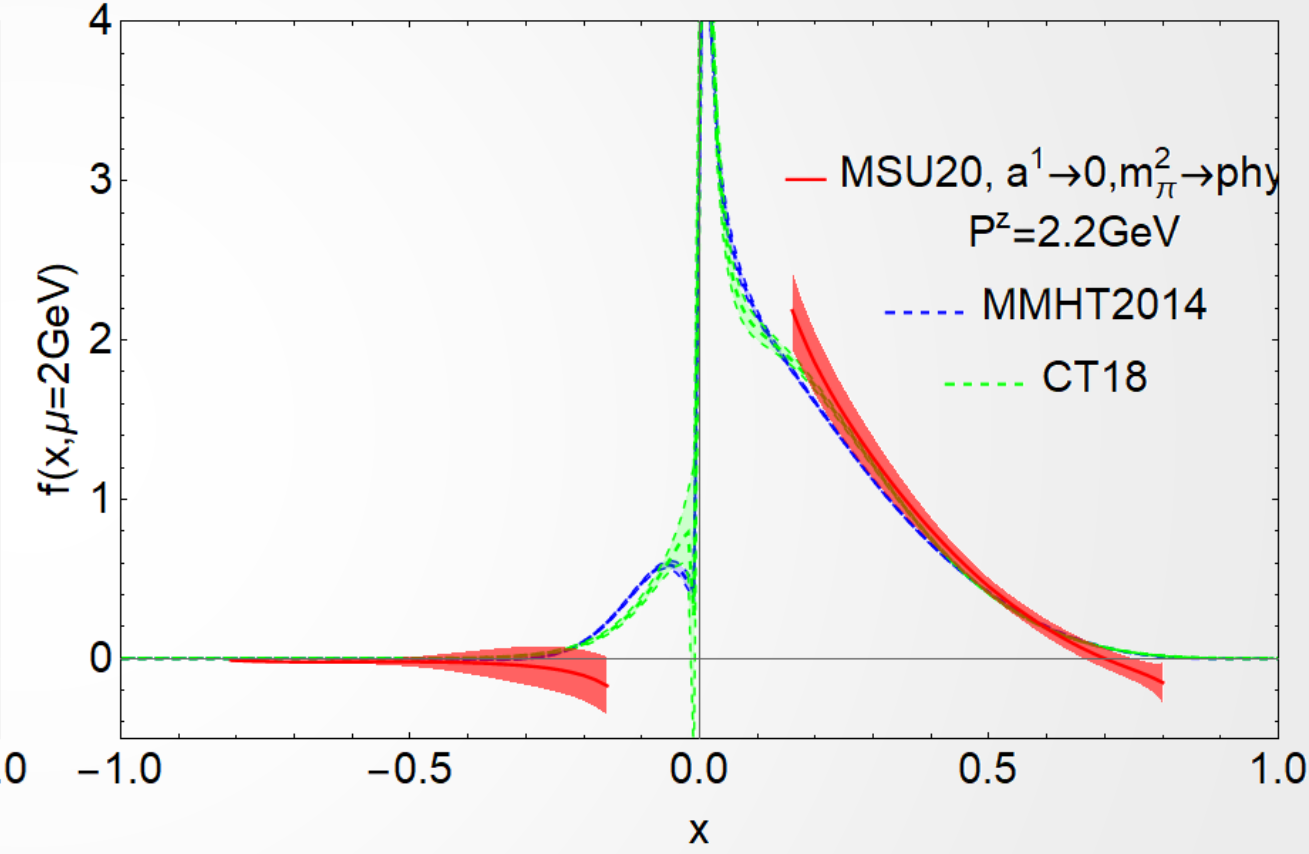

Comparing calibration ansatz

$$\tilde{h}(z, P^z) = \tilde{h}^R(z, P^z) e^{i\, z\, P^z \delta y}$$

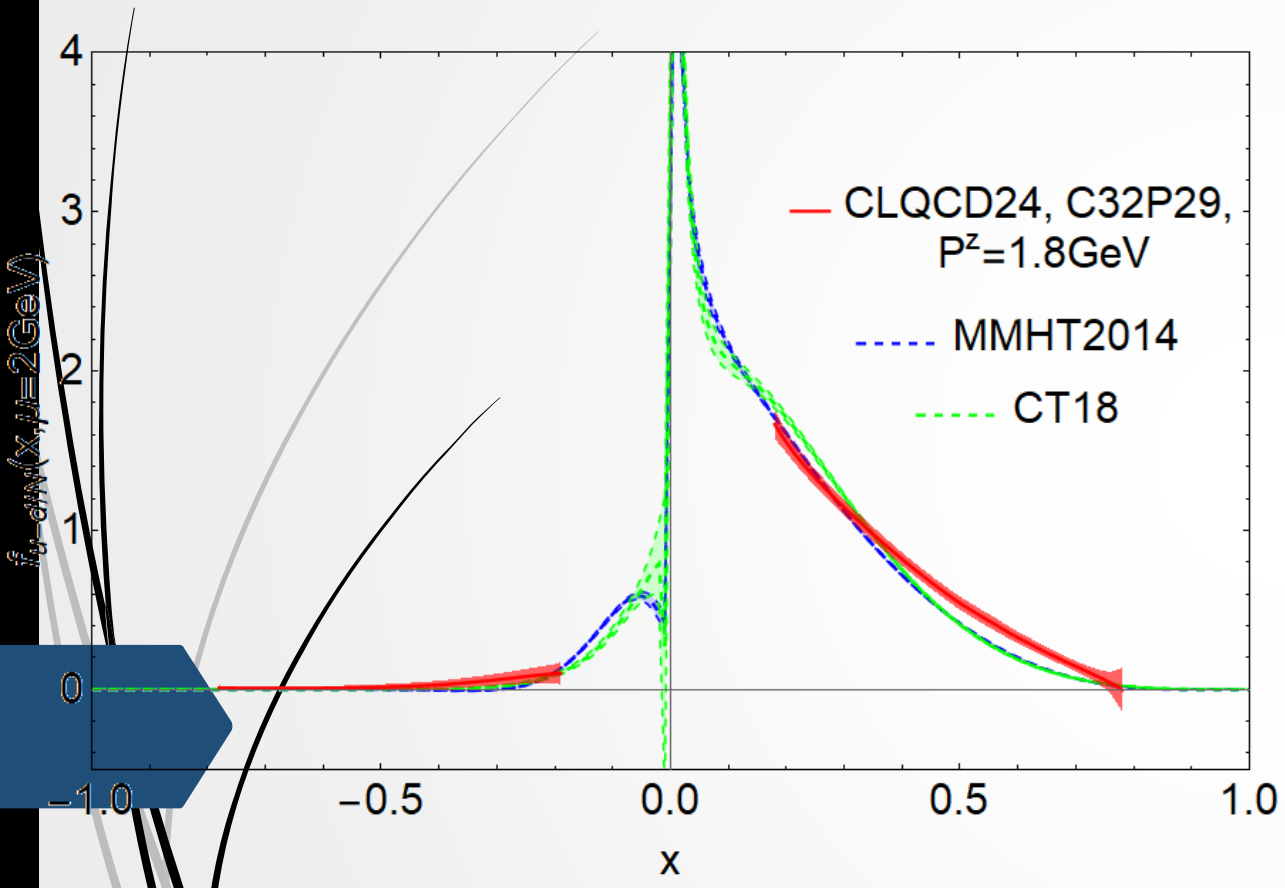

$$\tilde{h}(z, P^z) = \tilde{h}^R(z, P^z)(1 + i\, z\, P^z \delta y)$$

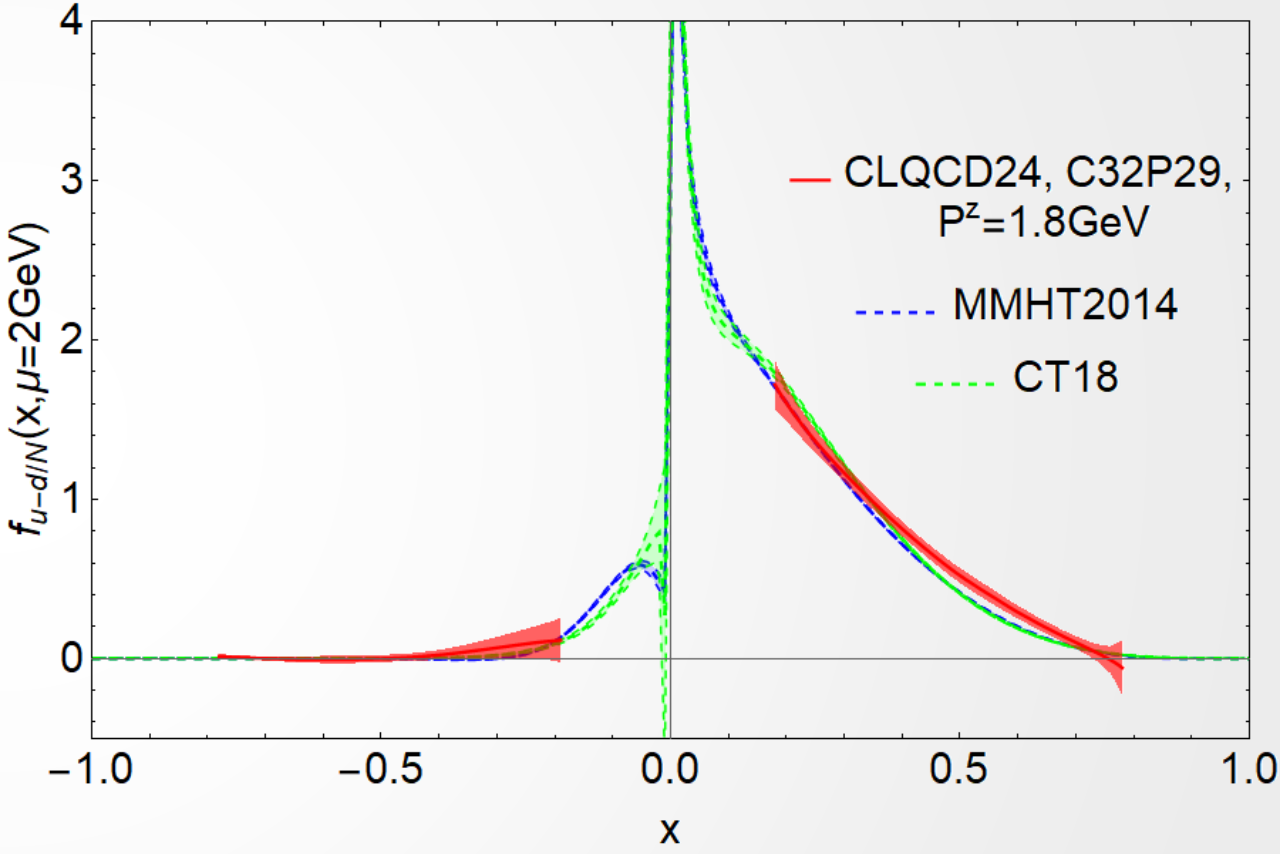

qPDFs obtained from different fit formulas

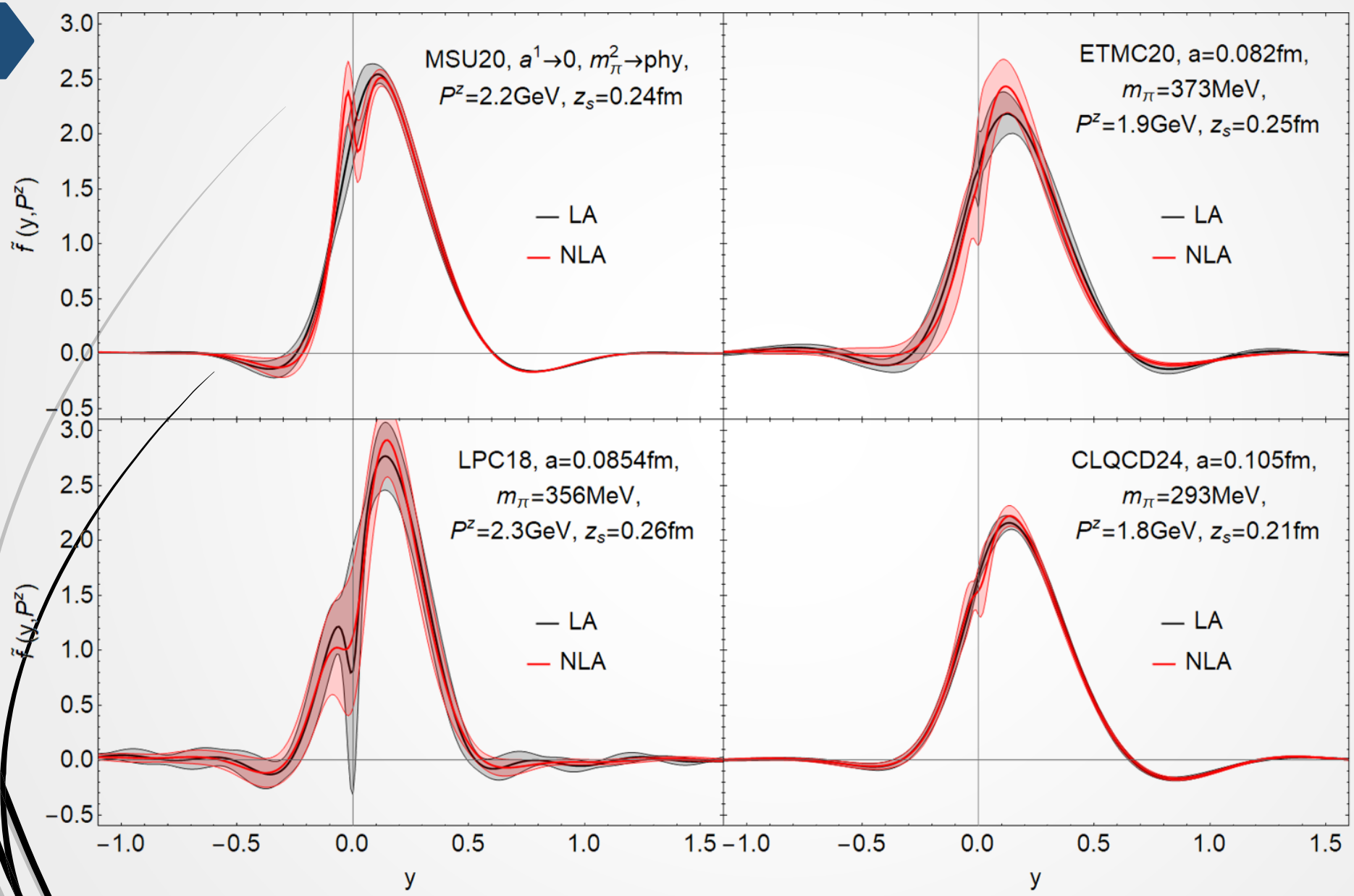

Fit range test

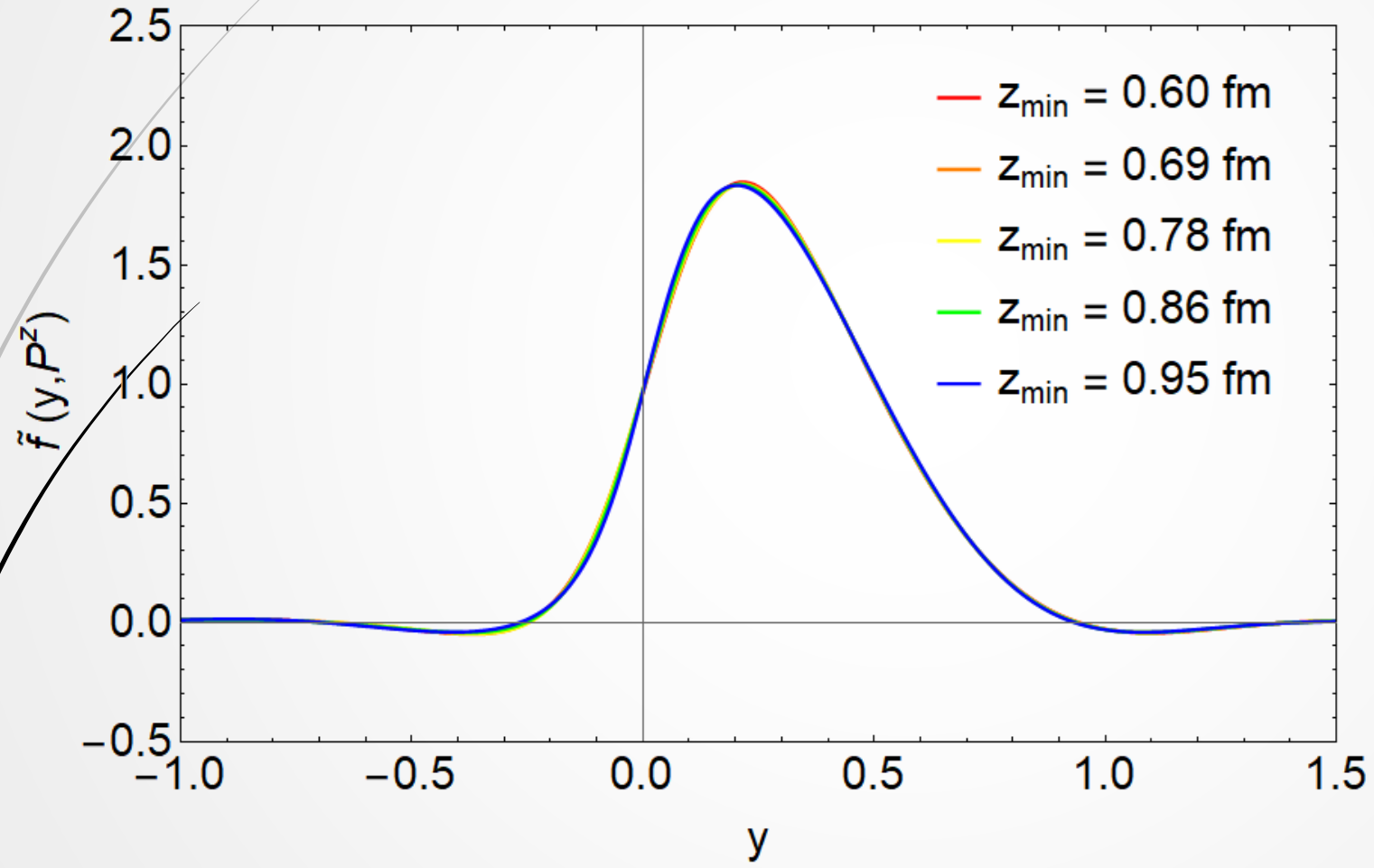

$z_{max} = 1.2fm$

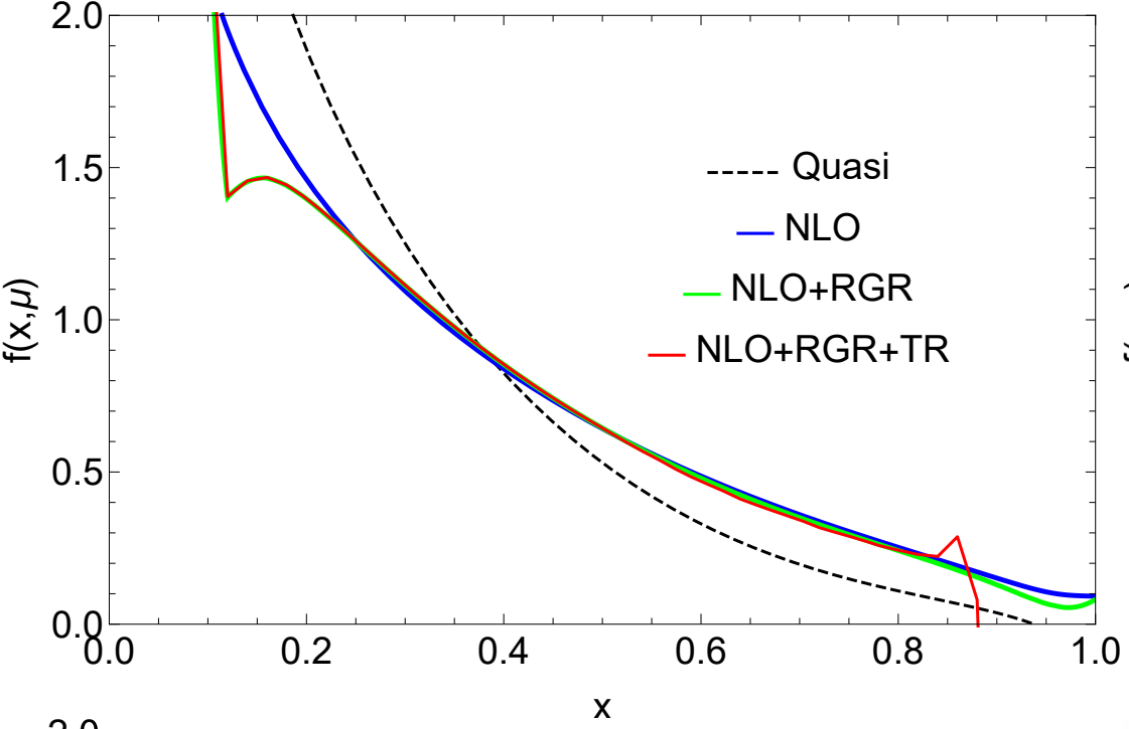
----- Quasi
NLO
NLO+RGR
NLO+RGR+TR
f(x,μ)
x

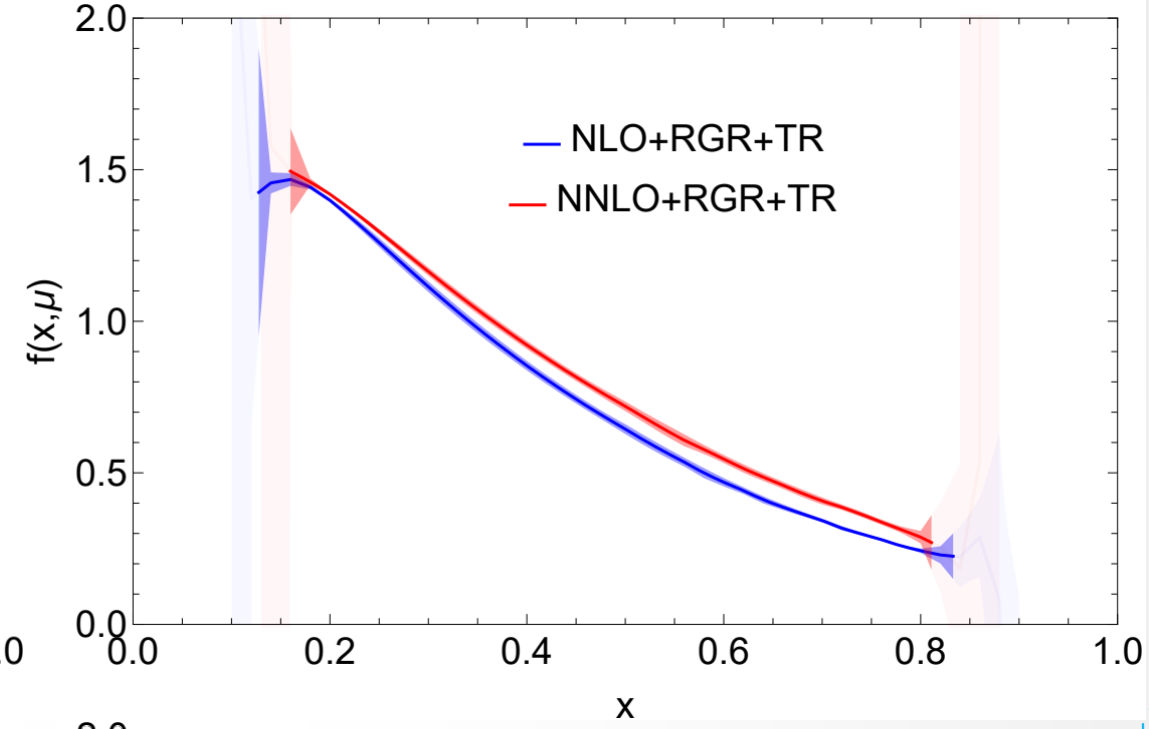
NLO+RGR+TR
NNLO+RGR+TR
f(x,μ)
x

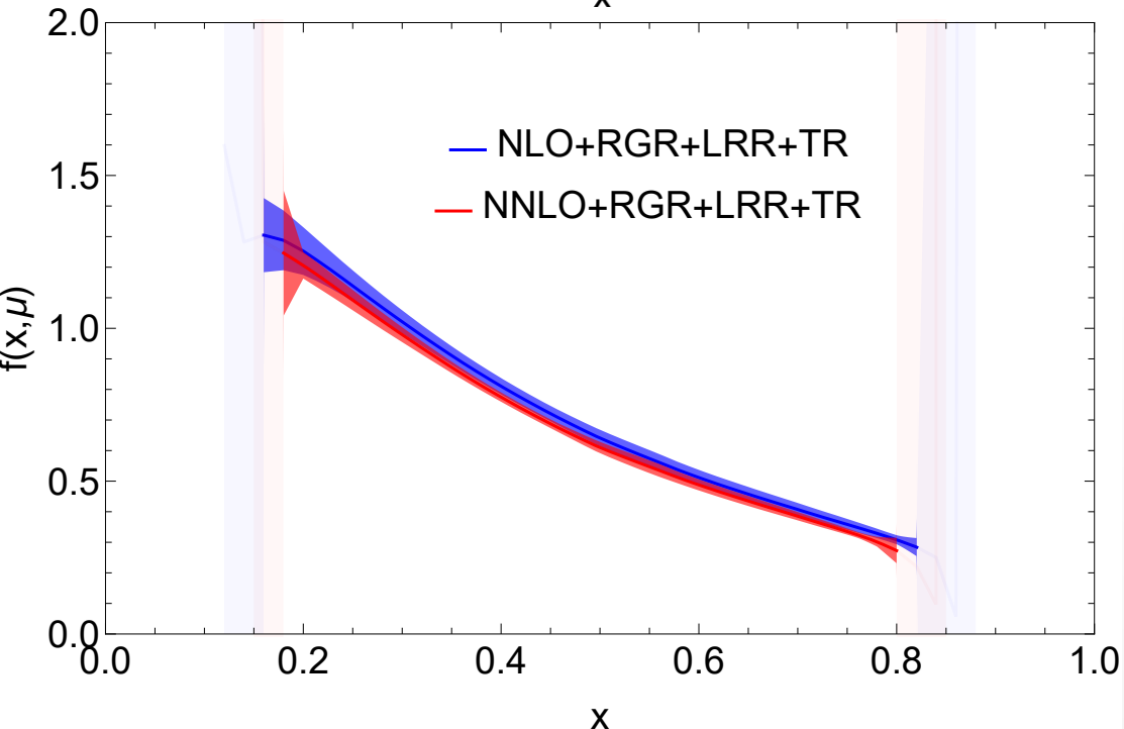
NLO+RGR+LRR+TR
NNLO+RGR+LRR+TR
f(x,μ)
x

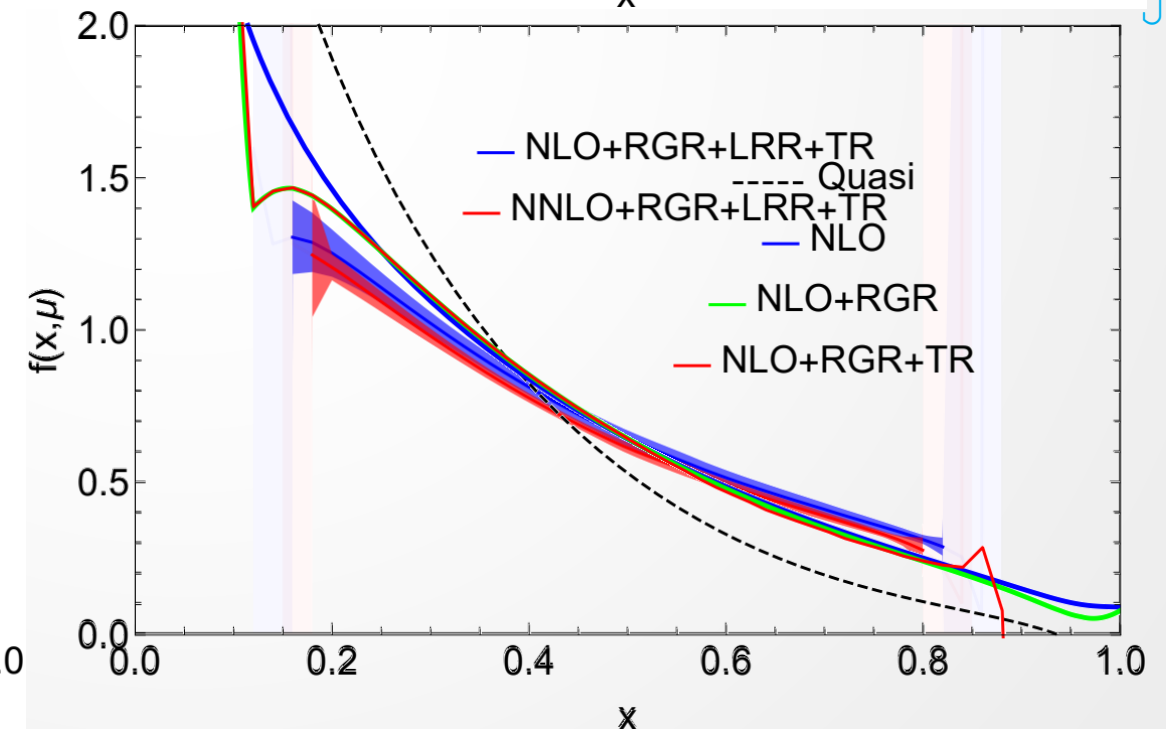
NLO+RGR+LRR+TR
----- Quasi
NNLO+RGR+LRR+TR
NLO
NLO+RGR
NLO+RGR+TR
f(x,μ)
x

Ji:2024hit

MSU20(Lin:2020fsj): result of each ensemble

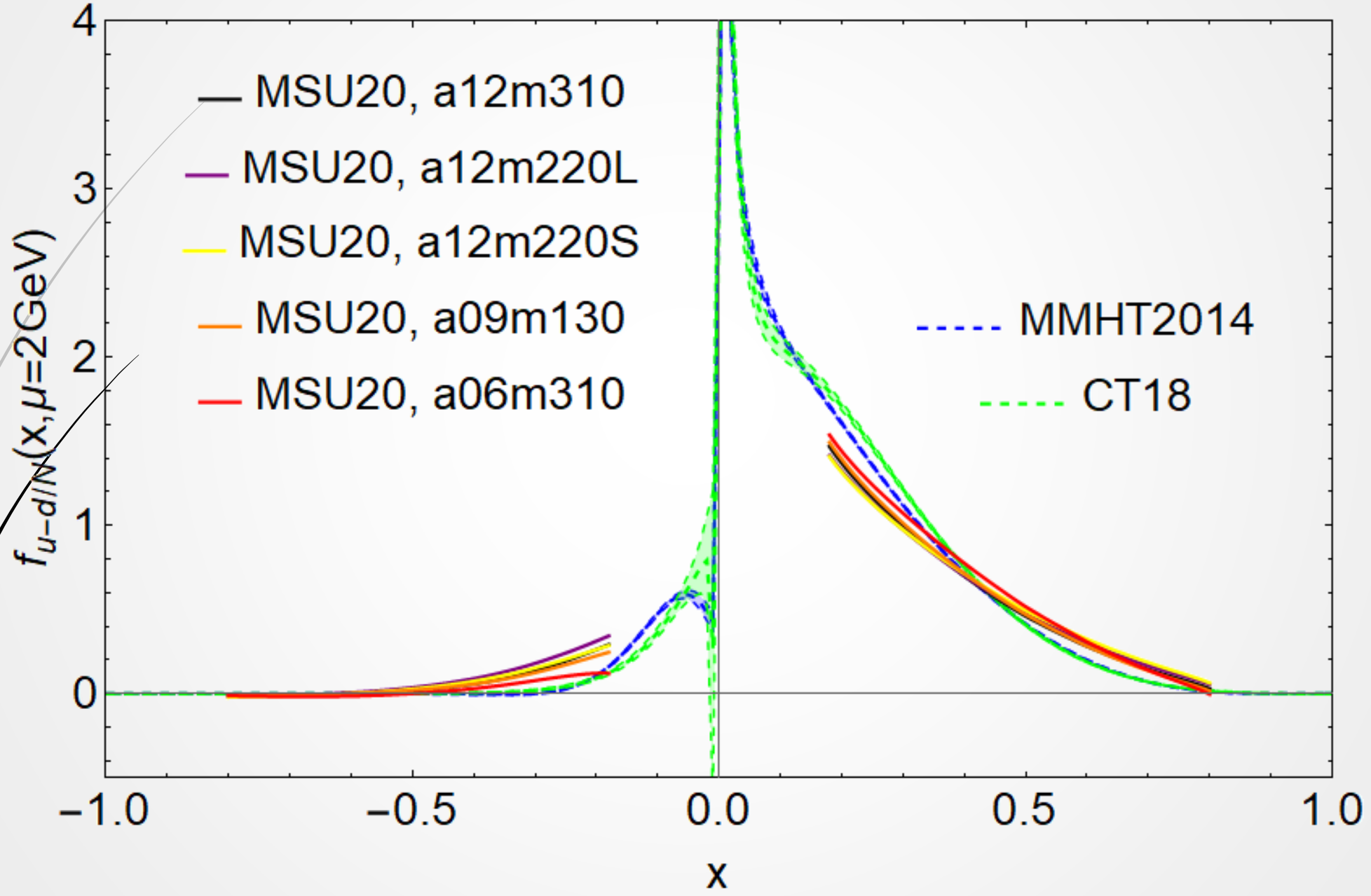

MSU20(Lin:2020fsj): coor extra (red) v.s. mom extra (black)

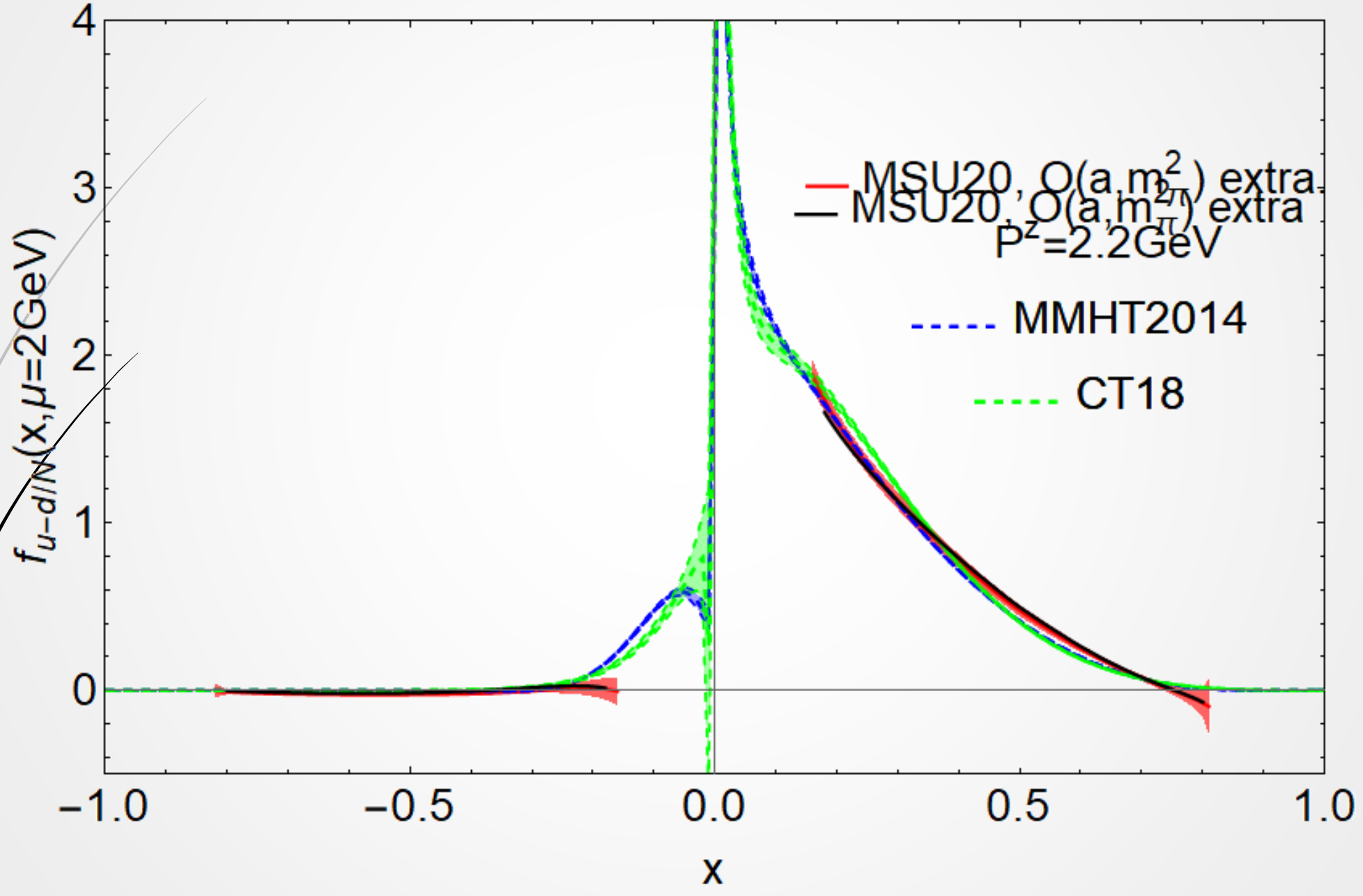

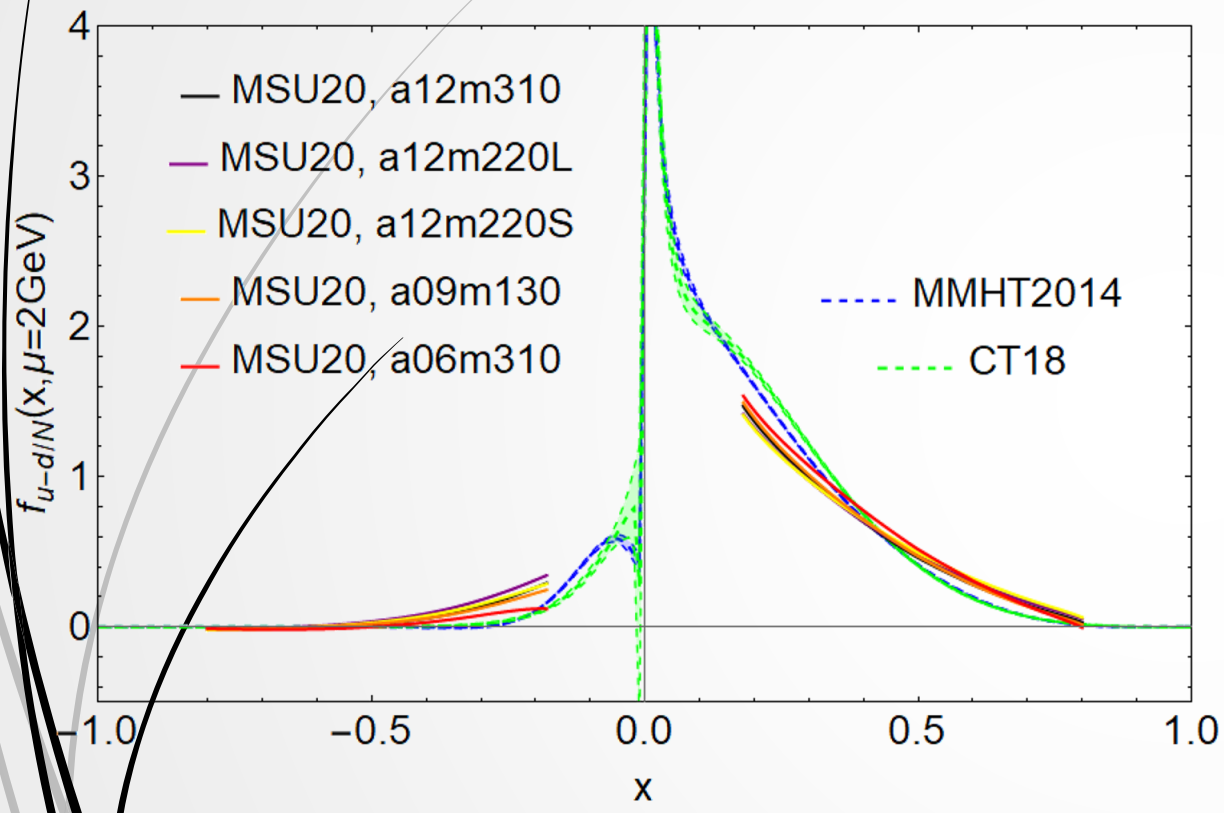
MSU20, a12m310
MSU20, a12m220L
MSU20, a12m220S
MSU20, a09m130
MSU20, a06m310
MMHT2014
CT18
$f_{u-d/N}(x,\mu=2GeV)$
x

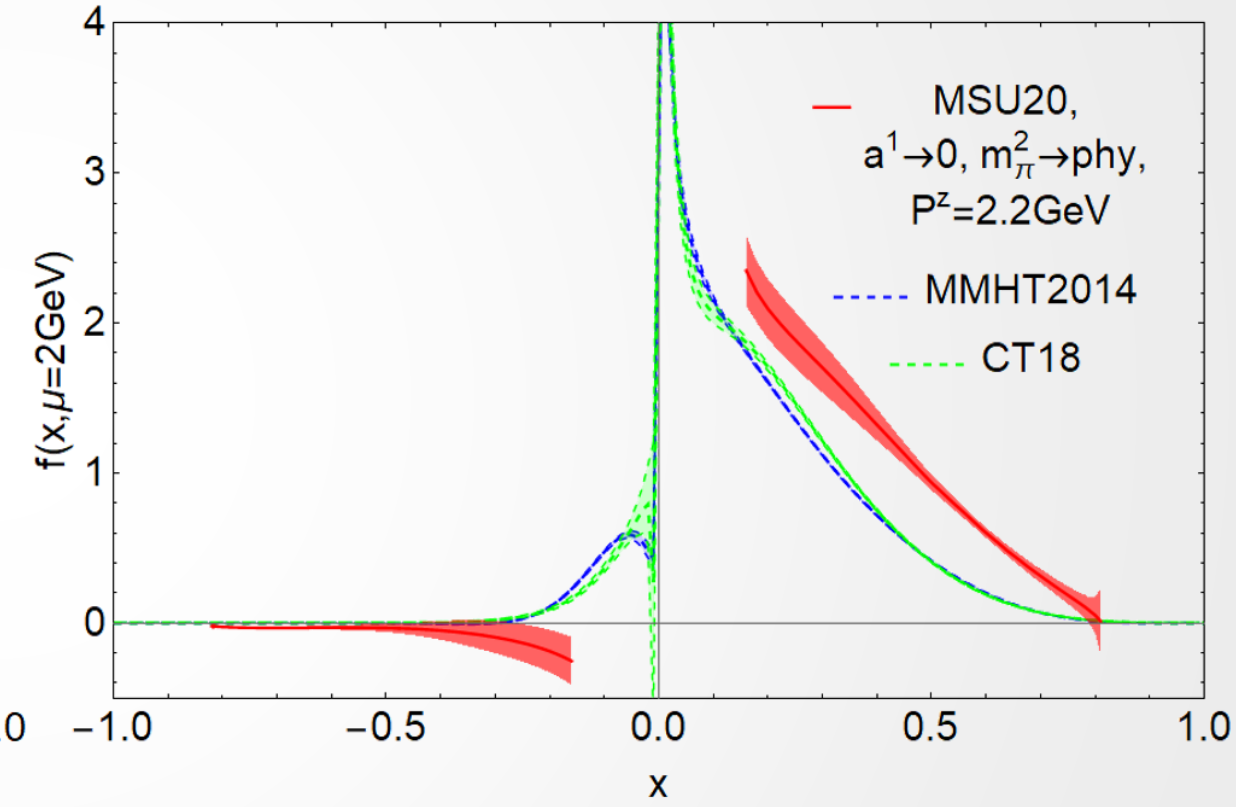
MSU20,
$a^1 \to 0$, $m_\pi^2 \to$ phy,
P^z=2.2GeV
MMHT2014
CT18
$f(x,\mu=2GeV)$
x

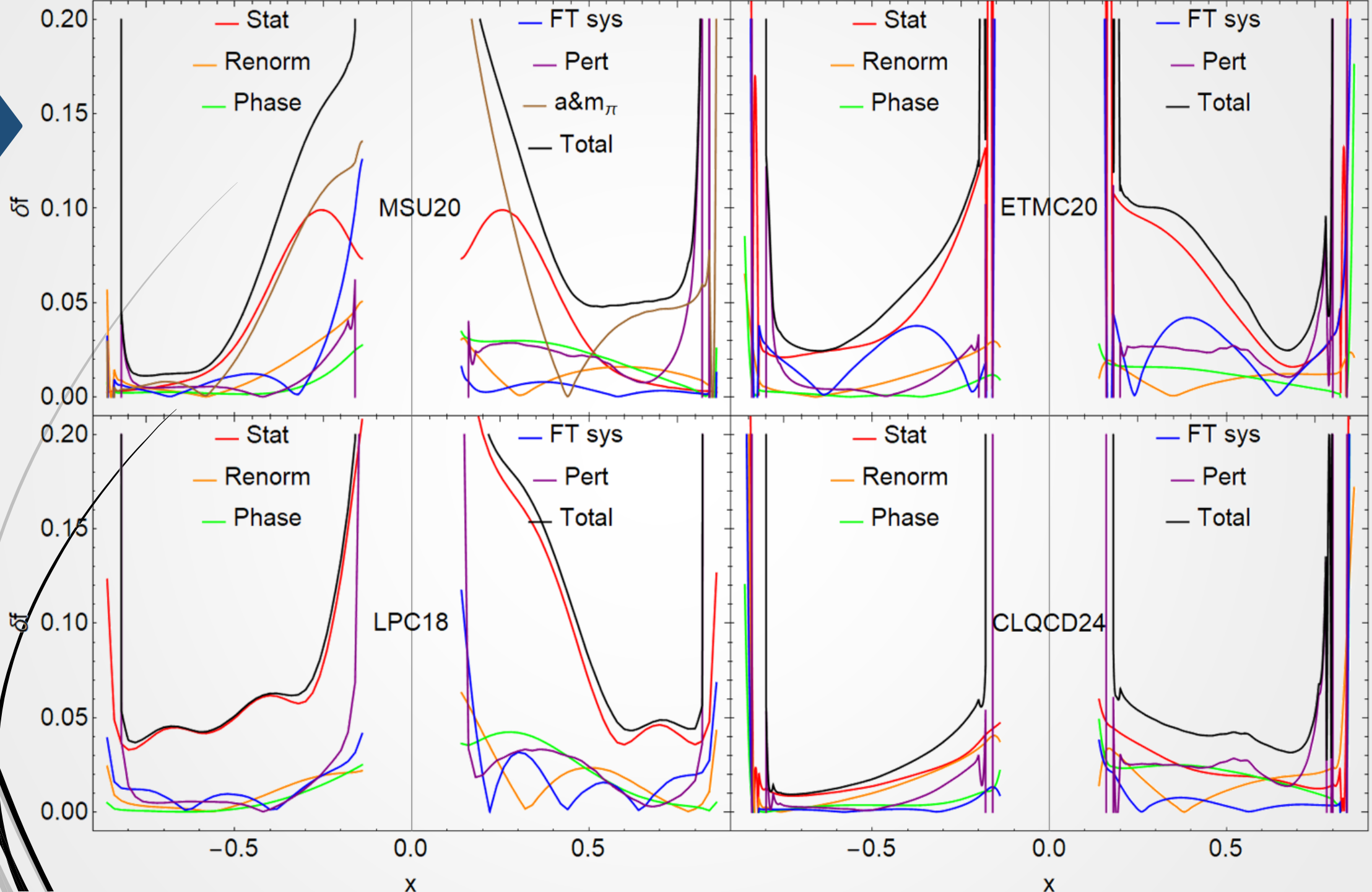
Stat
Renorm
Phase
FT sys
Pert
a&m$_\pi$
Total
MSU20
ETMC20
LPC18
CLQCD24
δf
x
0.20
0.15
0.10
0.05
0.00
−0.5
0.0
0.5